ROBUST AND ACCURATE CLASSICAL HOUGH TRANSFORM APPROACH FOR IRIS RECOGNITION

Thesis submitted in partial fulfillment of the requirements

for the award of degree of

Masters of Technology

In

Computer Science and Applications

Submitted by

Megha Chhabra

(601003015)

Under the supervision of

Dr. Amit Kumar

Assistant Professor

SCHOOL OF MATHEMATICS AND COMPUTER APPLICATIONS

THAPAR UNIVERSITY

PATIALA – 147004

JUNE 2012

CERTIFICATE

This is to certify that work presented in this thesis entitled "**Robust and accurate Classical Hough Transform approach for IRIS recognition**" in partial fulfillment of the requirements for the award of the degree of M.Tech (Computer Science & Applications) submitted in School of Mathematics and Computer Applications of Thapar University, Patiala, is an authentic record of my own work carried out under the supervision of Dr. Amit Kumar.

The matter presented in this thesis has not been submitted for the award of any other degree of this or any other university.

Megha Chhabra

Megha Chhabra

This to certify that above statement made by candidate is correct and true to the best of my knowledge.

Dr. Amit Kumar

Assistant Professor

School of Mathematics and Computer Applications

Thapar University

Patiala 147004

Countersigned by

Dr. S.S. Bhatia
Professor & Head, SMCA
Thapar University
Patiala

Dr. S.K. Mohapatra
Dean of Academic Affairs
Thapar University
Patiala

ACKNOWLEDGEMENT

Developing a software project is not easy task without the support and cooperation of number of people. First and foremost, I would like to express my sincere gratitude to my supervisor Dr. Amit Kumar, School of Mathematics and Computer Applications, Thapar University, Patiala, for his constant suggestions and encouragement all the time. He always provide motivating and enthusiastic environment to work with, it was great pleasure to do work under his supervision.

I would like to thank Prof. S. S. Bhatia, Head, School of Mathematics and Computer Applications, Thapar University, Patiala, for providing necessary facilities in the department to work.

I would like to thank my family for their fortitude. Without their support, nothing would have ever been possible. At the end I would like to thank God for providing me strength at the time of crises.

This acknowledgement would be incomplete if I do not mention the emotional support and blessings provided by Mr. Manjit Verma for his kind co-operation.

Megha Chhabra

(601003015)

ABSTRACT

As an important part of scientific community, object recognition has become admirably suitable facet of digital image processing. Circular objects are recurrently seen in many images. A large number of methods for circle detection have been studied for various industrial applications. The application province considered in this chapter is 'Iris recognition'. On the basis of earlier research and results, time comparison and the efficiency of various methods to detect iris in digital images are compared. Iris recognition is one such area which is loaded enough to research into and desires attention and upgrading. It is used in user verification security systems as well as in medical fields.

Iris recognition is based on the fact that the significant information for recognition is found within iris outline which is modeled as circle. Rest of the data from the eye region is redundant. Hough transform (HT) is an effective method for confirming the co-ordinates of the center of the circle and its radius. Circle Hough transform (CHT) provides a robust technique for iris detection, but the large amount of storage and computing complexity are the major drawbacks of it. Many modified versions have been applied by researchers in order to reduce computational complexity and memory requirements. Present work proposes a modified CHT which considerably improves the speed of the process without compromising the accuracy of the technique. An exhaustive analysis is conducted for a large number of iris images.

In order to achieve the objective, present work is proposing variations in CHT. The work is concerned with the time, computation and memory requirements of CHT. In a more extended version of chapter, information of valid region is exploited to develop appropriate method for speedy and correct extraction of circle. To reduce computation time, HT space is divided into equal sized four quadrants which lie in most probable area of the image to find circle center and radius. These quadrants contribute in finding the significant region of the image which needed to be processed. Hence, determining the valid region is the important step towards fast detection. This also permits limiting the memory needs of the algorithm. After that CHT is applied on all four extracted valid regions which give us fast recognition of the iris.

LIST OF TABLES

LIST OF FIGURES

TABLE OF CONTENTS

CHAPTER 1-INTRODUCTION

1.1 Overview

The first chapter briefly introduces the basics of images and edge detection. The second chapter provides an overview of various operators of detection of edges. This chapter also explains basics of HT based CHT method to detect circles. This chapter also introduces the anatomy of eye and application of eye (iris) detection in various fields. Chapter 3 describes the working of both CHT and modified CHT. Chapter 4 presents the output of the work done. Finally, concluding thesis in Chapter 5 with conclusion of the work done and evaluated results.

1.2 Basics of images

A digital image is a two-dimensional array of small square regions known as pixels [30]. In the case of a monochrome or gray-scale image, the intensity of each pixel is represented by a numeric value. It is also a representation of a two-dimensional image as a finite set of digital values, called picture elements or pixels. Digital images can be created by a variety of input devices and techniques:

- Digital cameras
- Scanners
- Coordinate measuring machines.

There are various types of digital images.

- Binary
- Grayscale
- Color

A binary image is a digital image that has only two possible values, 0 and 1, for each pixel. Binary images are also called bi-level or two-level. it is usually stored in memory

as a bitmap, a packed array of bits. Binary images often arise in digital image processing as masks or as the result of certain operations such as segmentation and thresholding.

Figure 1: A binary image.

Gray-scale images typically contain values in the range from 0 to 255, with 0 representing black, 255 representing white and values in between representing shades of gray.

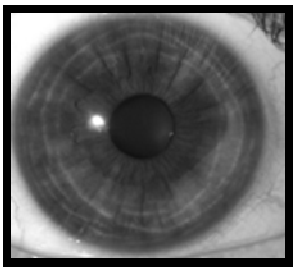

Figure 2: A gray scale image.

A color image can be represented by a two-dimensional array of Red, Green and Blue triples. Typically, each number in the triple also ranges from 0 to 255, where 0 indicates that none of that primary color is present in that pixel and 255 indicates a maximum amount of that primary color.

Figure 3 A colored image.

1.2.1 Type of image formats

There are two image main image file format definitions used in a typical graphic design project, Raster (or bitmap) images and vector images. Raster images are generally photographs or images made up of pixels. These images are resolution-dependent, meaning that their physical size is directly associated with their resolution (the number of Dots (pixels) per Square Inch or DPI that they contain).The most common image file formats are JPG, TIF, PNG, and GIF.

Digital cameras and web pages normally use JPG files because JPG compresses the data to be very much smaller in the file at the cost of image quality. However JPG uses lossy compression to accomplish this, which is a downside. This degree is selectable, to be lower quality smaller files, or to be higher quality larger files. In general today, JPG is rather unique in this regard, using lossy compression allowing very small files of lower quality, whereas almost any other file type is lossless (and larger). JPG is used when small file size is more important than maximum image quality (web pages, email, camera memory cards, etc). But JPG is good enough in many cases, if we don't overdo the compression. Perhaps good enough for some uses even if we do overdo it (web pages, etc). But if you are concerned with maximum quality for archiving your important images, then you do need to know two things: 1) JPG should always choose higher Quality and a larger file, and 2) do not keep editing and saving your JPG images repeatedly, because more quality is lost every time you save it as JPG

TIF is lossless (including LZW compression), which is considered the highest quality format for commercial work. The TIF format is not necessarily any “higher quality” (the image pixels are what they are), but there simply are no additional losses or artifacts to degrade and detract. And TIF is the most versatile, except that web pages don't show TIF files, because some browsers do not show TIF images. For other purposes however, TIF does most of anything you might want, from 1-bit to 48-bit color, RGB, CMYK, LAB, or Indexed color.

GIF was designed by CompuServe in the early days of computer 8-bit video, before JPG, for video display at dial up modem speeds. GIF is lossless, but it is always an indexed color file (8-bits, 256 colors maximum), and is poor for 24-bit color photos. Don't use

GIF for color photos today, the color is too limited. But GIF is still very good for web graphics (i.e., with a limited number of colors). For graphics of only a few colors, GIF can be much smaller than JPG, with more clear pure colors than JPG).

PNG can replace GIF today, and PNG also offers many options of TIF too (indexed or RGB, 1 to 48-bits, etc). One additional feature of PNG is transparency for 24 bit RGB images. Normally PNG files are a little smaller than TIF LZW (both use lossless compression, of different types), but PNG is perhaps slightly slower to read or write.

1.2.2 Comparison between various formats

Table 1 demonstrates the comparison between various format types of images.

Table 1: Comparison between formats of an image.

	Color data mode -bits per pixel
JPG	RGB - 24-bits (8-bit color), Grayscale - 8-bits (only these)
TIF	Versatile, many formats supported. Mode: RGB or CMYK or LAB, and others, almost anything. 8 or 16-bits per color channel, called 8 or 16-bit “color” (24 or 48-bit RGB files). Grayscale - 8 or 16-bits, Indexed color - 1 to 8-bits, Line Art (bi-level) - 1-bit.
PNG	RGB - 24 or 48-bits (called 8-bit or 16-bit “color”), Grayscale - 8 or 16-bits, Indexed color - 1 to 8-bits,
GIF	Indexed color - 1 to 8-bits (8-bit indexes, limiting to only 256 colors maximum.) Color is 24-bit color, but only 256 colors.

Present code works for tiff format. TIFF - Tag Image File Format (.TIF file extension) is the format of choice for archiving important images. TIFF is THE leading commercial

and professional image standard. TIFF is the most universal and most widely supported format across all platforms, Mac, Windows, Unix. Data up to 48 bits is supported.

TIFF supports most color spaces. TIFF is a flexible format with many options. The data contains tags to declare what type of data follows. New types are easy to invent, and this versatility can cause incompatibly, but about any program anywhere will handle the standard TIFF types that we might encounter. This choice improves efficiency (speed), but all major programs today can read TIFF either way, and TIFF files can be exchanged without problem.

TIFF supports most color spaces. TIFF is a flexible format with many options. The data contains tags to declare what type of data follows. New types are easy to invent, and this versatility can cause incompatibly, but about any program anywhere will handle the standard TIFF types that we might encounter. This choice improves efficiency (speed), but all major programs today can read TIFF either way, and TIFF files can be exchanged without problem.

TIFF supports most color spaces. TIFF is a flexible format with many options. The data contains tags to declare what type of data follows. New types are easy to invent, and this versatility can cause incompatibly, but about any program anywhere will handle the standard TIFF types that we might encounter. This choice improves efficiency (speed), but all major programs today can read TIFF either way, and TIFF files can be exchanged without problem.

For photographic images, TIFF image files can use LZW lossless compression. Lossless means there is no quality loss due to compression. Lossless guarantees that you can always read back exactly what you thought you saved, bit-for-bit identical, without data corruption. This is a critical factor for archiving master copies of important images. Most image compression formats are lossless, with JPG and Kodak PhotoCD PCD files being the main exceptions.

LZW is most effective when compressing solid indexed colors (graphics), and is less effective for 24 bit continuous photo images. Featureless areas compress better than detailed areas. LZW is more effective for grayscale images than color. LZW is often

counter-productive for 48 bit images; the 16 bit TIF file using LZW will probably be considerably larger than one with no compression.

Tiff is the standard universal format for high quality images; it simply does the best job the best way. Give TIF very major consideration, both for photos and documents, especially for archiving anything where quality is important.

But TIF files for photo images are generally pretty large. Uncompressed TIFF files are about the same size in bytes as the image size in memory. Regardless of the novice view, this size is a plus, not a disadvantage. Large means lots of detail, and it's a good thing. 24 bit RGB image data is 3 bytes per pixel. That is simply how large the image data is, and TIF LZW stores it with recoverable full quality in a lossless format.

1.3 Edge detection

Present work is concerned with the detection of circle features. The detection result should be robust and accurate in real time. To achieve these, the edge detection algorithms are used to satisfy some criteria:

(1) Proper detection

(2) Unique edge response

(3) Low computational complexity

(4) Robustness.

The first two criteria ensure that an edge is unique, which helps to reduce the computation and maintain a good accuracy.

Many edge detection methods have been developed, such as Sobel, Canny etc they usually produce multi responses or time wasting.

Edge detection refers to the process of identifying and locating sharp discontinuities in an image. The discontinuities are the abrupt changes in pixel intensity which characterize boundaries of objects in a scene. Classical methods of edge detection involve convolving the image with a two dimensional (2-D) operator, which is constructed to be sensitive to

large gradients in the image while returning values of zero in uniform regions. There are large numbers of edge detection operators available, each designed to be sensitive to certain types of edges. Variables involved in the selection of an edge detection operator include:

- Edge orientation: The geometry of the operator determines a characteristic direction in which it is most sensitive to edges. Operators can be optimized to look for horizontal, vertical, or diagonal edges.
- Noise environment: Edge detection is difficult in noisy images, since both the noise and the edges contain high-frequency content. Attempts to reduce the noise result in blurred and distorted edges. Operators used on noisy images are typically larger in scope, so they can average enough data to discount localized noisy pixels. This results in less accurate localization of the detected edges.
- Edge structure: Not all edges involve a step change in intensity. Effects such as refraction or poor focus can result in objects with boundaries defined by a gradual change in intensity. The operator needs to be chosen to be responsive to such a gradual change in those cases. Newer wavelet-based techniques actually characterize the nature of the transition for each edge in order to distinguish, for example, edges associated with hair from edges associated with a face.

There are many ways to perform edge detection. However, the majority of different methods may be grouped into two categories:

- Gradient: The gradient method detects the edges by looking for the maximum and minimum in the first derivative of the image.
- Convolution: The convolution is performed by sliding the kernel over the image, generally starting at the top left corner, so as to move the kernel through all the positions.

1.4 Literature survey

Edge detection is a potential move in pattern recognition of digital images. The goal of the edge detection process in a digital image is to determine the frontiers of all represented objects. Several algorithms have been proposed to accomplish this task. Traditional algorithms use high spatial frequency filtering followed by thresholding of the resulting strength map, differential, or template-matching operators such as Sobel, Prewitt, Krisch, Robinson, and Roberts etc. Some edge detectors attempt to enhance edges by filtering or involve fitting a model or a function to image surface while others use morphological properties of images to detect edges. First-order linear filters constitute the algorithms most widely applied to edge detection in digital images. In the literature studied so far, it has been concluded that the major problem with traditional gradient based or filtering based algorithm is that those in the process of removing noise most of the time smoothen out the edges and boundaries in the image making it difficult to extract that important information later on.

Hough transform [1] has long been recognized as a technique of almost unique promise for shape and motion analysis in images containing noisy, missing, and extraneous data but its implementation has been deliberate due to its computational and storage complexity and the lack of a detailed understanding of its properties. The detection of circular and elliptic shapes is a common task of HT. The Hough transform is a well known technique for detecting parametric curves in images. This algorithm has many applications in the real world which makes it a potential area for research. Shearer & kitchen [3] presented an efficient algorithm for filling gaps in the voting procedure for a Hough transform caused by quantization effects. These gaps adversely affect peak detection. This also described improvement of same in any number of dimensions. Walsh & Raftery [4] proposed an algorithm in which Simple clustering methods provide good identification of curve parameters with the removal of noise parameters which is achieved via a simple thresholding of the importance weights. Fernandes & Olivera [8] successfully introduced an improved voting scheme for the HT that allows a software implementation to achieve real-time performance even for relatively large images. The

approach clustered approximately collinear edge pixels and, for each cluster, casts votes for a reduced set of lines in the parameter space, based on the quality of the fitting of a straight line to the pixels of the cluster. This improvement not only significantly improved the performance of the voting scheme, but also produced a much cleaner voting map and made the transform more robust to the detection of spurious lines. Cha et al. [5] developed a new extension to the HT by intensifying the Hough space by a third parameter, the horizontal or vertical coordinate of the image space, to provide incremental information as to the length of the linear feature being sought. Therefore, short lines can now be more easily detected. They have also used a Bayesian probabilistic approach that additionally enlarged the precision of extended Hough transform. Zhao et al. [9] proposed a new algorithm in which the HT is only employed in column-pair spaces of large-scale microarray data, to reduce the computational complexity. Lu & Tan [10] developed an iterative randomized Hough transform (IRHT) for recognition of incomplete ellipses in images with strong noise. The advantage of using IRHT is iterative parameter adjustments and the reciprocal use of the image and parameter spaces.

Shekhar et al. [6] described a novel method to automatically localize the optic disk using HT. A circular region of interest was found by first isolating the brightest area in the image by means of morphological processing, and then the Hough transform was used to detect the circular feature of the optical disk, hence reducing the time of computation. Cheng et al. [18] presented a method in which an eliminating particle swarm optimization (EPSO) algorithm was employed to reduce the time consumption of HT. The parameters of the solution after Hough transformation were considered as the particle positions, and the EPSO algorithm searched the optimum solution by eliminating the weakest particles which speed up the computation. Smereka & Duleba [11] introduced an effective method for circular object recognition like nuclei of cells, which showed robustness for irregularities and for disturbances like noise. In addition to it, Singh et al. [12] conducted an analysis of time complexity on various stages of skew detection process by a preprocessing stage using a simplified form of block adjacency graph (BAG),followed by voting process using the Hough transform and then de-skewing the image using rotation. Gall & Lempitsky [16] introduced the Hough forests approach for object detection by

building discriminative class-specific part appearance codebooks based on random forests that cast probabilistic votes within the Hough transform framework. Apart from the accuracy, the use of random forests potentially allows a very time efficient implementation. Du & Yang [13] demonstrated a robust and highly accurate method for detecting the radiation center of a single circular or rectangular field. Method employed the sub pixel accuracy of the HT method which depends on prior knowledge of the field shapes and reduced statistical variance due to averaging information from multiple pixels. Guo et al. [17] presented an idea to suppress the impact of noise edges on accumulation of votes in Hough space produced by complex background or texture regions in images. Surround suppression is employed to allocate different weights to votes of different edges according to the region in which they are located. Peaks formed by noise edges are thus lowered compared with those formed by clear edges, which often give the boundaries between different objects of interest. Maji & Malik [14] introduced the Hough transforming discriminative framework which leads to improved accurateness by allowing the local parts to vote for possible transformations of the object hence allowing use of the peaks of the voting space for importance sampling of windows for further evaluation. Lehmann et al. [27] added a research in literature by producing better detection by using Principled Implicit Shape Model (PRISM) which interprets Hough voting as a dual implementation of linear sliding window detection. It also explained how to avoid soft-matching and spatial pyramid descriptors during detection without losing their positive effect, hence making algorithms simpler and faster. Knopp et al. [22] proposed 3D use of Hough transform. Authors introduced 3D SURF features in combination with the probabilistic Hough voting framework for the purpose of 3D shape class recognition. Bhatia & Chhabra [23] described a method for enhancing the speed of extracting circle i.e. iris from the image by extracting a valid region from the image, using circle Hough transform. This not only reduced the image storage and the quantity of operations, it also improved the speed of the process, without compromising the accuracy of the technique. A modified version of Hierarchical Hough transform was also proposed which further reduced the time taken to detect iris. Borrmann et al. [20] proposed a novel accumulator design, whose cells were of equal size. This property leads to an easier detection of planes when using the Hough Transform. The proposed

accumulator is compared to previously known designs as well. Tu et al. [25] discovered the self-similarity in HT butteries. Based on this property a simple method was proposed to obtain a very high resolution HT without the limitations associated with peak splitting and vote spreading. Hough transform has been accompanied with many techniques in order to improve the results to be followed from the intended application.

Reina et al. [7] proposed an algorithm that used a robust Hough transform enhanced by fuzzy reasoning to estimate the angle of inclination of the wheel trace with respect to the vehicle reference frame. In addition to it, Izadinia et al. [19] proposed a new method, namely Fuzzy Generalized Hough Transform (FGHT), in which a set of fuzzy rules were referred by the gradient direction of edge pixels and vote for the probable position of the center. Additionally, the proposed method could identify the boundary of the rotated and scaled object via a new voting strategy with least error under various conditions. Mokhayeri & Akrbarzadeh [26] proposed a system in which the eye region is detected using the genetic algorithm (GA), and a fuzzy filter is designed for noise reduction. Edge detection was performed based on fuzzy reasoning and linking was done using Hough transform. Then relevant features extracted of an eye using signal processing technique, were imported into the learning system to classify the active states between stress and relaxed condition of eye. Fuzzy systems are not preferred with HT when the application province is time consuming.

CHAPTER 2-CLASSICAL HOUGH TRANSFORM

2.1 Edge detection techniques

2.1.1 Sobel's operator

The Gradient of an Image $I(x, y)$ at location (x, y) is the vector

$$G = G_x i + G_y j \qquad (2.1.1)$$

Where G_x and G_y are partial derivative of $I(x, y)$ in x and y direction respectively.

This operator consists of a pair of 3×3 convolution kernels as shown in Figure 4. One kernel is simply the other rotated by 90°.

-1	0	+1
-2	0	+2
-1	0	+1

Gx

+1	+2	+1
0	0	0
-1	-2	-1

Gy

Figure 4: Sobel's operator

These kernels are designed to respond maximally to edges running vertically and horizontally relative to the pixel grid, one kernel for each of the two perpendicular orientations. The kernels can be applied separately to the input image, to produce separate measurements of the gradient component in each orientation. These can then be combined together to find the absolute magnitude of the gradient at each point and the orientation of that gradient. The gradient magnitude is given by:

$$G = ((G_x)^2 + (G_y)^2)^{1/2} \qquad (2.1.2)$$

Typically, an approximate magnitude is computed using:

$$|G| = |G_x| + |G_y| \qquad (2.1.3)$$

which is much faster to compute.

The angle of orientation of the edge (relative to the pixel grid) giving rise to the spatial gradient is given by:

$$\theta = \tan^{-1}(G_y / G_x) \qquad (2.1.4)$$

(a) **(b)**

Figure 5: a) Original image, b) Sobel operator on original image.

2.1.2 Robert's cross operator:

The Roberts Cross operator performs a simple, quick to compute, 2-D spatial gradient measurement on an image. Pixel values at each point in the output represent the estimated absolute magnitude of the spatial gradient of the input image at that point.

The operator consists of a pair of 2×2 convolution kernels as shown in Figure 6. One kernel is simply the other rotated by 90°. This is very similar to the Sobel operator.

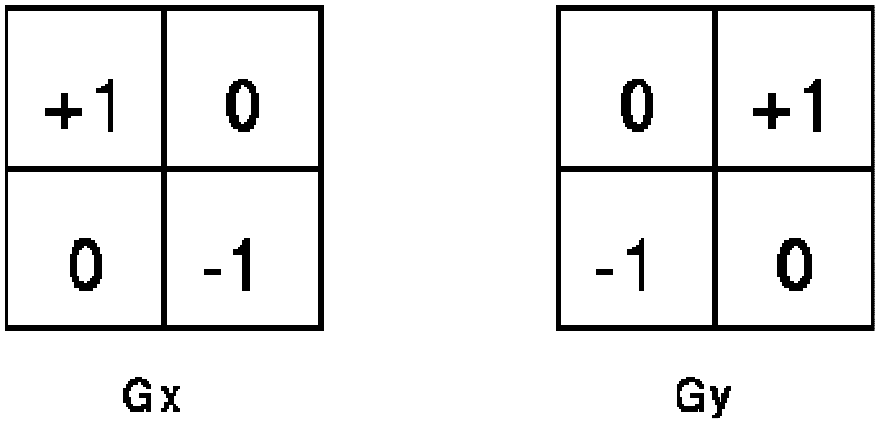

Figure 6: Robert's cross operator .

These kernels are designed to respond maximally to edges running at 45° to the pixel grid, one kernel for each of the two perpendicular orientations. The kernels can be applied separately to the input image, to produce separate measurements of the gradient component in each orientation (call these G_x and G_y). These can then be combined together to find the absolute magnitude of the gradient at each point and the orientation of that gradient. The gradient magnitude is given by:

$$|G| = \sqrt{G_x^{\,2} + G_y^{\,2}} \qquad (2.1.5)$$

Although typically, an approximate magnitude is computed using:

$$|G| = |G_x| + |G_y| \qquad (2.1.6)$$

which is much faster to compute.

The angle of orientation of the edge giving rise to the spatial gradient (relative to the pixel grid orientation) is given by:

$$\theta = \arctan(G_y / G_x) - 3\pi/4 \qquad (2.1.7)$$

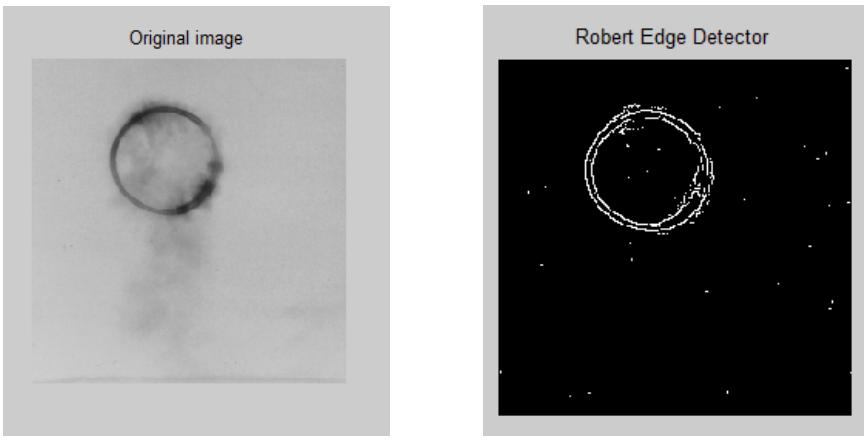

(a) **(b)**

Figure 7: a) Original image; b) Robert operator on original image.

2.1.3 Prewitt's operator:

Prewitt operator is similar to the Sobel operator and is used for detecting vertical and horizontal edges in images.

$$h_1 = \begin{bmatrix} 1 & 1 & 1 \\ 0 & 0 & 0 \\ -1 & -1 & -1 \end{bmatrix} \quad h_2 = \begin{bmatrix} -1 & 0 & 1 \\ -1 & 0 & 1 \\ -1 & 0 & 1 \end{bmatrix}$$

Figure 8: Prewitt's operator

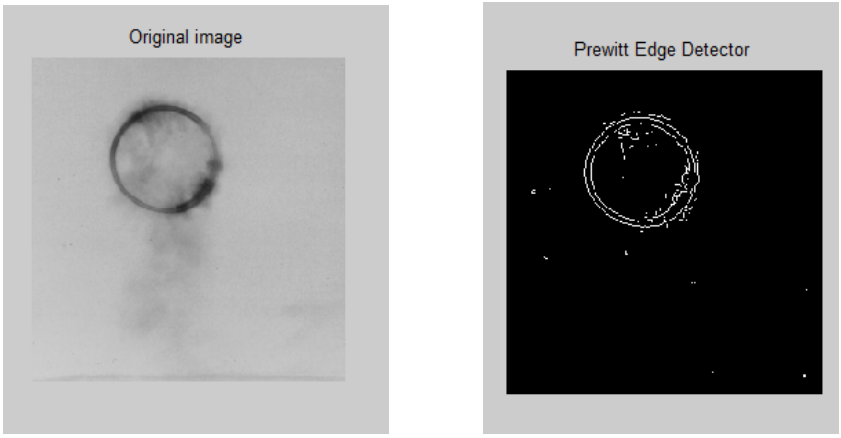

(a) **(b)**

Figure 9: a) Original image; b) Prewitt operator on original image.

2.1.4 Canny's operator

The Canny edge detection algorithm is known to many as the optimal edge detector. In this operator, a list of criteria is used to improve current methods of edge detection. The

first and most obvious is low error rate. It is important that edges occurring in images should not be missed and false edges must not be given as output. The second criterion is that the edge points be well localized. A third criterion is to have only one response to a single edge.

Based on these criteria, the canny edge detector first smoothes the image to eliminate and noise. It then finds the image gradient to highlight regions with high spatial derivatives. The algorithm then tracks along these regions and suppresses any pixel that is not at the maximum (non maximum suppression). The gradient array is now further reduced by hysteresis. Hysteresis is used to track along the remaining pixels that have not been suppressed. Hysteresis uses two thresholds and if the magnitude is below the first threshold say T1, it is set to zero (made a non edge). If the magnitude is above the high threshold say T2, it is made an edge. And if the magnitude is between the 2 thresholds, then it is set to zero unless there is a path from this pixel to a pixel with a gradient above T2.

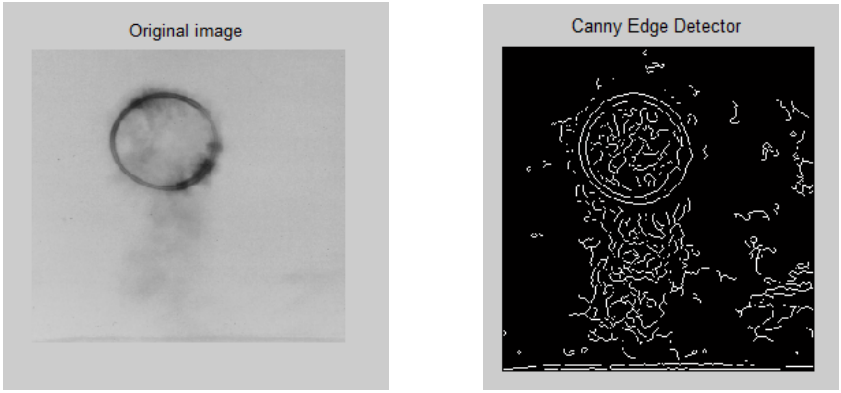

(a) (b)

Figure 10: a) Original; b) Canny operator on original image.

2.1.5 Performance of edge detection algorithms

- Gradient-based algorithms such as the Prewitt filter have a major drawback of being very sensitive to noise. The size of the kernel filter and coefficients are fixed and cannot be adapted to a given image. An adaptive edge-detection algorithm is necessary to provide a robust solution that is adaptable to the varying noise levels of these images to help distinguish valid image contents from visual artifacts introduced by noise.

- Canny edge detection algorithm is computationally more expensive compared to Sobel, Prewitt and Robert's operator. However, the Canny's edge detection algorithm performs better than all these operators under almost all scenarios.

2.2 Classical Hough Transform

The HT is a method which can be used to separate facets of a particular shape within an image. CHT is most commonly used for the detection of regular curves such as lines, circles, ellipses, etc. A *generalized* Hough transform can be employed in applications where a simple analytic description of a feature(s) is not possible. The generalized Hough transform is computationally complex relative to Classical Hough Transform.

Despite its domain restrictions, the Classical Hough Transform retains many applications, as most manufactured parts and many anatomical parts investigated in medical imagery, contain feature boundaries which can be described by regular curves. The main advantage of the Hough transform technique is that it is tolerant of gaps in feature boundary descriptions and is relatively unaffected by image noise.

The Hough transform can be used to classify the parameter(s) of a curve which best fits a set of given edge points. This edge description is commonly obtained from a feature detecting operator such as http://homepages.inf.ed.ac.uk/rbf/HIPR2/roberts.htmRoberts Sobel or Canny edge detector and may be noisy, *i.e.* it may contain multiple edge fragments corresponding to a single whole feature. Furthermore, as the output of an edge detector defines only where features are in an image, the work of the Hough transform is to determine both what the features are (i.e. to detect the feature(s) for which it has a parametric (or other) description) and how many of them exist in the image.

Detecting lines and circles in an image is a fundamental issue in image processing applications. Extracting circles from digital images has received more attention for several decades because an extracted circle can be used to yield the location of circular object in many industrial applications. So far many circle-extraction methods have been developed. The Circle Hough transform (CHT) [4] is one of the best-known algorithms and aims to find circular shapes with a given radius r within an image. Usually edge map of the image is calculated then each edge point contributes a circle of radius to an output

accumulator space. For unknown circle radii, the algorithm should be run for all possible radii to form a 3-dimensional parameter space, where two dimensions represent the position of the center, and the third one represents the radius. The output accumulator space has a peak where these contributed circles overlap at the center of the original circle. Giving output as center co-ordinates and radius of circle corresponding to the maximum peak, circle around original iris is drawn using bresenham's circle drawing method.

2.3 Human eye Anatomy

Eye is like a camera. The external object is seen like the camera takes the picture of any object. Light enters the eye through a small hole called the pupil and is focused on the retina, which is like a camera film. Eye also has a focusing lens, which focuses images from different distances on the retina. The colored ring of the eye, the iris, controls the amount of light entering the eye. It closes when light is bright and opens when light is dim. A tough white sheet called sclera covers the outside of the eye. Front of this sheet (sclera) is transparent in order to allow the light to enter the eye, the cornea. Ciliary muscles in ciliary body control the focusing of lens automatically. Choroid forms the vascular layer of the eye supplying nutrition to the eye structures. Image formed on the retina is transmitted to brain by optic nerve. The image is finally perceived by brain. A jelly like substance called vitreous humor fill the space between lens and retina. The lens, iris and cornea are nourished by clear fluid, aqueous humor, formed by the ciliary body and fill the space between lens and cornea. This space is known as anterior chamber. The fluid flows from ciliary body to the pupil and is absorbed through the channels in the angle of anterior chamber. The delicate balance of aqueous production and absorption controls pressure within the eye.

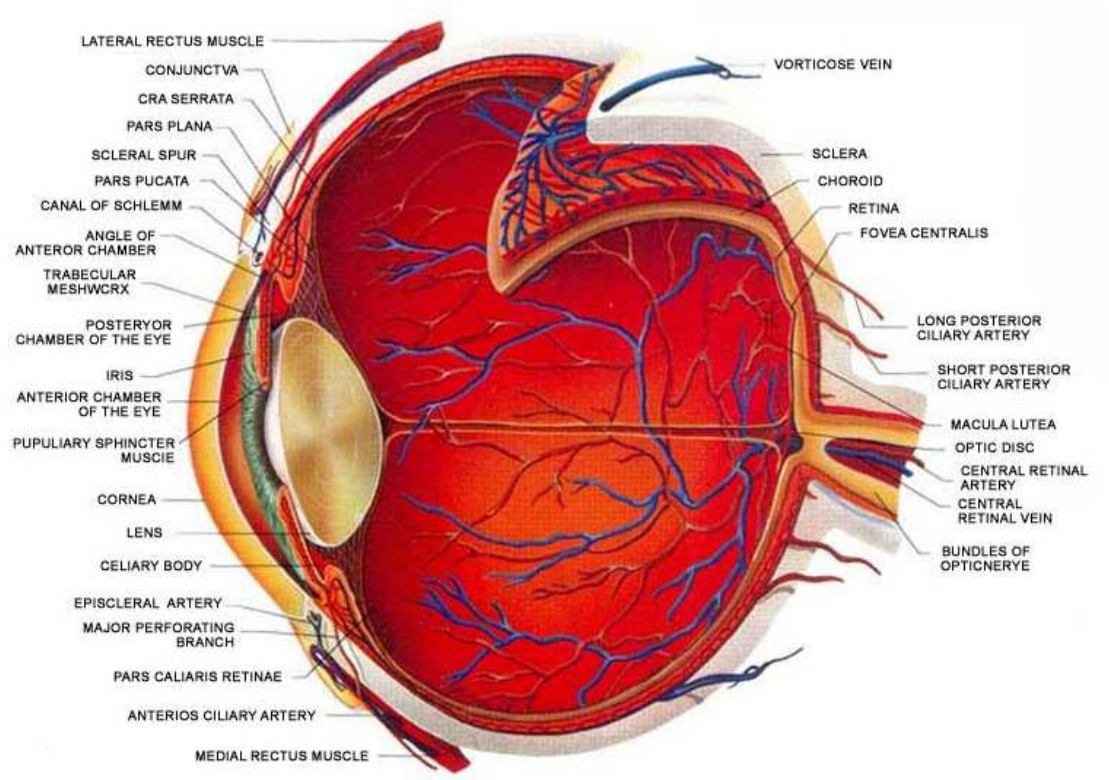

Figure 11: Structure of Human eye.

Good eye health and eye care are crucial to the value of sight. Some of the most common eye diseases and conditions are Glaucoma refers to a group of eye diseases that affect the optic nerve and may cause vision loss. Cataract is a painless condition where the normally clear aspirin-sized lens of the eye starts to become cloudy. The result is much like smearing grease over the lens of a camera, which impairs normal vision. Age-related macular degeneration is an eye disease with onset usually after age 60 that progressively destroys the macula, the central portion of the retina, impairing central vision. It rarely causes blindness because only the center of vision is affected. A retinal detachment is a separation of the retina from its attachments to its underlying tissue within the eye. Most retinal detachments are a result of a retinal break, hole, or tear. Once the retina has torn, liquid from the vitreous gel passes through the tear and accumulates behind the retina. The buildup of fluid behind the retina is what separates (detaches) the retina from the back of the eye. Uveitis is defined as all inflammatory processes of the middle layers of the eye, also called the uveal tract or uvea. The uvea is very important because its many veins and arteries transport blood to the parts of the eye that are critical for vision.

Symptoms and signs of uveitis may include eye redness and irritation, blurred vision, eye pain, increased sensitivity to light, and floating spots. Potential causes include infection with a virus, fungus, bacteria or parasite, inflammatory disease affecting other parts of the body, or injury to the eye. Severe allergic eye symptoms can be very distressing and are a common reason for visits to the allergist or ophthalmologist. Occasionally, severe eye allergies cause serious damage that can threaten eyesight. Most corneal ulcers are caused by infections and can be bacterial (common in people who wear contact lenses), viral (herpes simplex virus and varicella virus), or fungal (improper care of contact lenses or overuse of eyedrops that contain steroids). Symptoms include red eyes, pain; feeling like something is in the eye, tearing, pus/thick discharge, blurry vision, pain from bright lights, swollen eyelids, or a white or gray round spot on the cornea. A sty is a tender, painful red bump located at the base of an eyelash or inside the eyelid. A sty results from an acute infection of the oil glands of the eyelid that occurs after these glands have become clogged. A sty also may arise from an infected hair follicle at the base of an eyelash.

Eyes or specifically, Iris Recognition is a high-confidence biometric identification system with promising future in the security systems area. Its robustness and unobtrusiveness, as opposed to most of the currently deployed systems, make it a good candidate to replace most of the security systems around. Iris recognition is a combination of image processing and computer vision.

The iris in Figure 12 is the colored part of the eye. The iris controls light levels inside the eye similar to the aperture on a camera. The round opening in the center of the iris is called the pupil.

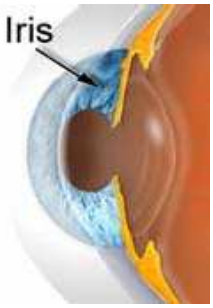

Figure 12: The Human iris

Personal identification has been the interest of many researches in the field of pattern recognition and machine learning due to the increasing demand for a highly reliable secure environment. Many biometric identification technologies such as facial recognition, fingerprint recognition, voice recognition, and iris recognition come to meet those demands.

Facial recognition faces many problems since face itself is a 3D object that varies depending on the angle, pose, illumination, and age.

Figure 13: Iris recognition: Reliable secure environment

Iris, on the other hand, begins to form in the third month of gestation, and the structures creating its patterns become unchangeable in two or three years. Furthermore, the iris pattern does not correlate with genetic determination since its forming depends on the initial environment of the embryo, which yields to the fact that even the left and the right irises for the same person are not identical. Add to this the fact that the iris is isolated and protected from external environment. Besides, it is impossible to surgically modify the iris without unacceptable risk to vision. Finally, its physiological response to light provides one of several natural tests against artifice.

Therefore, and due to its unique and rich properties, iris recognition comes to be the Iris recognition has been an active research area in the last years, due its high accuracy and the encouragement of both the government and private entities to replace traditional security systems, which suffer of noticeable margin of error. However, early research was obstructed by the lack of iris images.

Figure 14: Facial recognition, palm recognition, eye recognition.

Iris recognition is based on the fact that the human iris contains unique features that completely distinguish a person; the actual information we are looking for is found within the iris patterns. Thus, it is logical that in implementing such a biometric system requires isolating the iris region from the other parts of the image, which are of no relevance. The iris region is approximated by a ring, defined by the iris/sclera boundary and the iris/pupil boundary. Thus, we should be able to detect these boundaries and isolate the part of the image within.

The first step in recognizing the valid region involves distinguishing, approximately, the valid region from the invalid region. Owing to limited resources available, we can only get circles with irregular edge. In reality, the valid region is a regular circle. In order to avoid processing, the invalid region in subsequent phases is removed.

Valid region recognition has the merits to the later processing:

(1) Storage quantity is much less than before. As invalid region is removed, the storage space the images occupy is reduced greatly and the image transmission amount is reduced.

(2) Faster operational speed is achieved as a result of the reduction of the number of pixels being processed. The program operation speed boosts up subsequently.

(3) The quality of imaging processing is improved.

In spite of its popularity owing to its simple theory of operation, the CHT has some disadvantages when it works on a discrete image. The large amount of storage and computing power required by the CHT are the major disadvantages of using it in real-time applications.

CHAPTER 3-PROBLEM STATEMENT AND SOLUTION

3.1 Classical Hough Transform

Detecting iris (circle) using CHT includes simple Hough Transform method. CHT is easy to understand but takes large computational time.

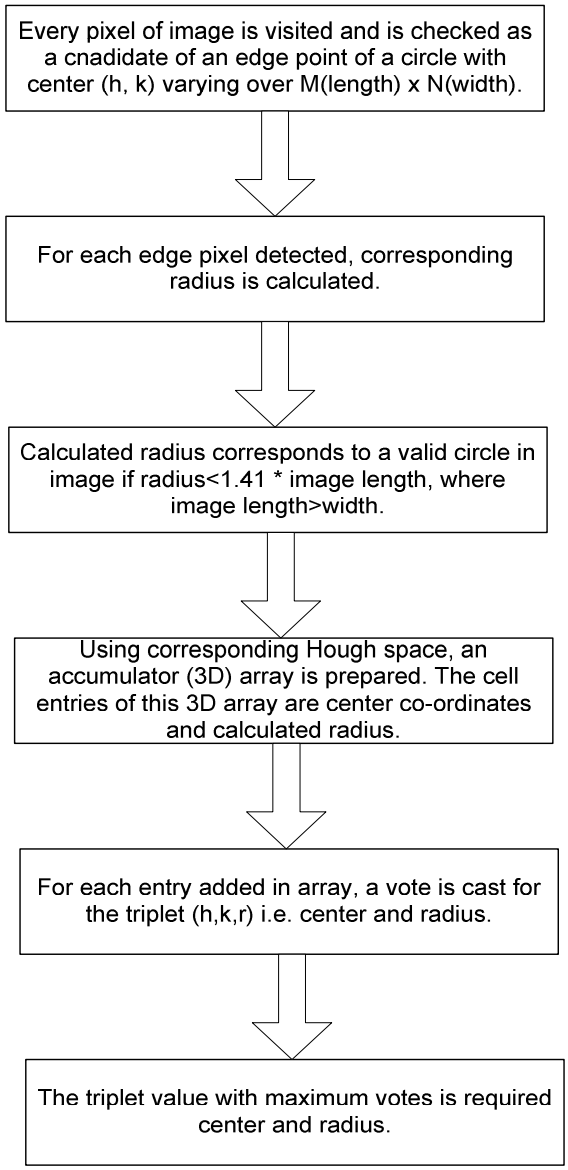

Figure 15: Graphical representation of Classical Hough Transform

Following are the steps to detect circle using Classical Hough Transform:

Step1: In order to detect circle, equation of a circle is given by:

$$(x-h)^2+(y-k)^2=r^2 \qquad (3.1.1)$$

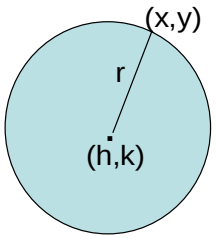

Figure 16: Circle with center (h, k) and radius r.

Where (x, y) is set of all points on circle, r is radius and (h, k) is center of circle

With a given gray scaled image $f(x, y)$ of size $M \times N$, every pixel of it is visited and is checked as a candidate of an edge point of a circle with center (h, k) varying over image's $\text{length}(M) \times \text{width}(N)$.

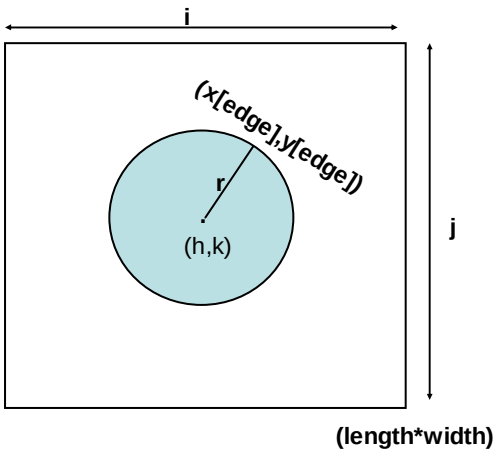

Figure 17: An image representing relation between edge points and image length and width.

Step 2: For each edge point in image, corresponding radius is calculated.

$$r = sqrt((i - xedge[t])^2 + (j - yedge[t])^2) \qquad (3.1.2)$$

where $0 < t <$ number of edge points, $0 < i <$ image width, $0 < j <$ image length .

This radius must lie inside edges of image. Using the values of corresponding center co-ordinates and radius, an accumulator array [3D] is prepared as

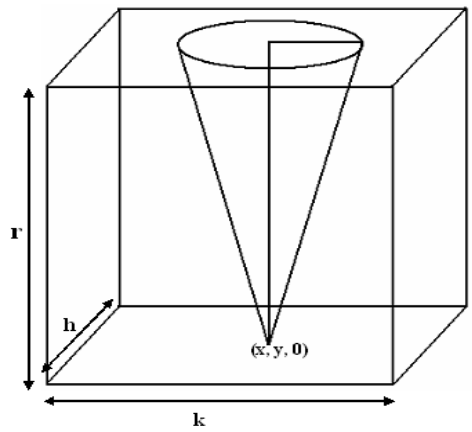

Figure 18: Hough space for CHT

Step 3: In this array, cell values contain accumulated votes for each center coordinate and corresponding radius generated. This calls for a circle in the image as required circle (or iris) which contains maximum value in array. Using every value of pixel of image and edge points, the radii calculated gives a peak. Apart from local maxima, the required radius with maximum votes lies at global maxima and that value is displayed as center co-ordinates and radius as (h_0, k_0, r_0) of required circle (iris).

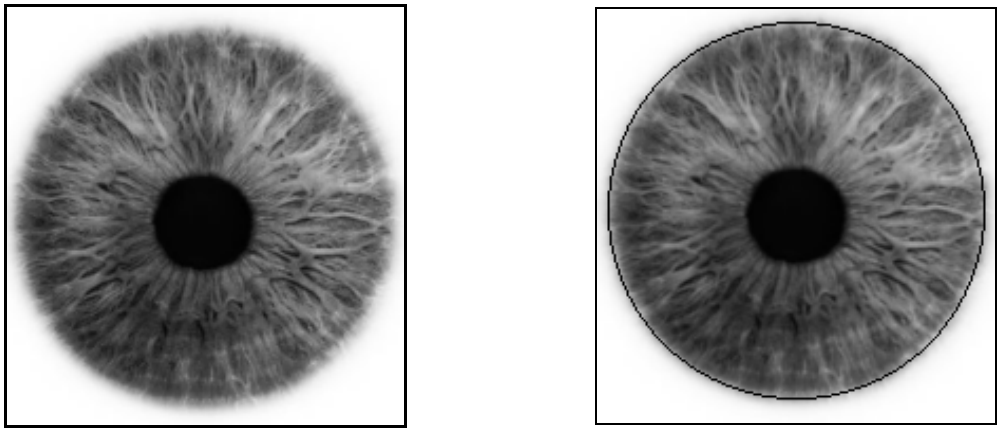

(a) (b)

Figure 19: (a) Captured image of iris, (b) Detected iris from image

CHT uses every pixel of image and that makes it store almost every pixel and process it. This results in easy processing of image. Also it results in large computational time for detection and large memory storage area for data to be processed for same.

So, *CHT is quite easy in implementation whereas takes large computational time and storage area. In other words, CHT visits pixels which may not give any useful results.*

3.2 Modified Circle Hough Transform

In case of HT based detection methods execution speed is directly proportional to the number of edge pixels in the input image. The proposed method reduces the number of image edge pixels to be processed. Reduction in time of execution of programs to extract circle from image is the basic and probably most important feature of this work. In order to achieve this objective, present work emphasizes on the various ways in which number of pixels to visit may get reduced.

The motive is achieved in two steps:

- Limiting the image space to the valid region.
- Apply transforms on the valid region extracted.

Further, limiting the image space is achieved in following steps:

- Transform the image into HT space.
- Divide the HT space into a four quadrants. These quadrants are of maximum probability to find suitable and accurate results.

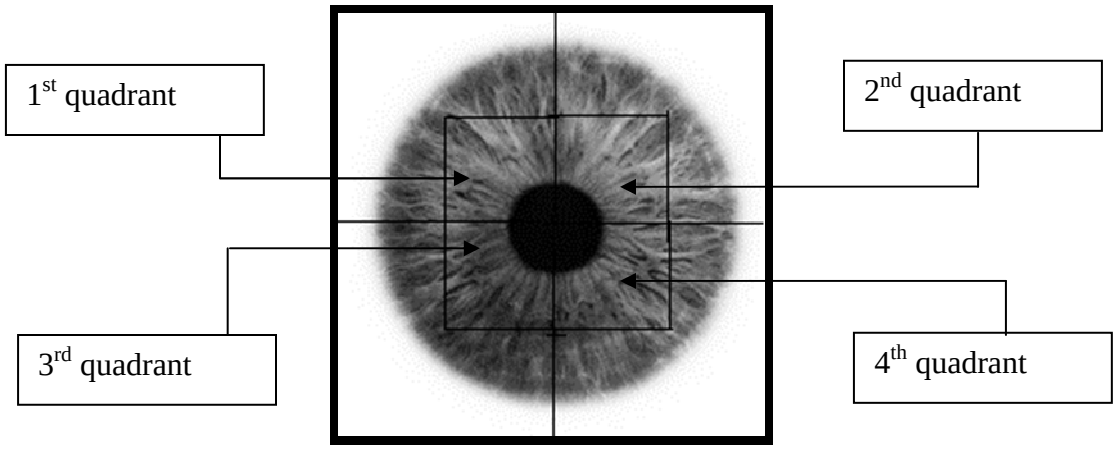

Figure 20: Equal sized quadrants.

Determining valid region to process out of whole space provided is first and an important step for fast extraction of circle. Presently, four equal sized grids are constructed in HT space as shown in Figure 21. The purposes of these quadrants are:

- To use most probable areas of image from where center and radius of iris at any side of image can be find out in faster way.
- To reduce number of pixels to process.

This work comprises of analysis of time of execution of this improved transform and comparison of same with existing CHT. The basic idea behind the use of relatively smaller area in HT space of CHT transform is to analyze the fact that without compromising the accuracy of detection of iris and reducing the number of pixels to visit, whether it still performs efficiently or not. Following Figure 22 shows the algorithm of modified CHT.

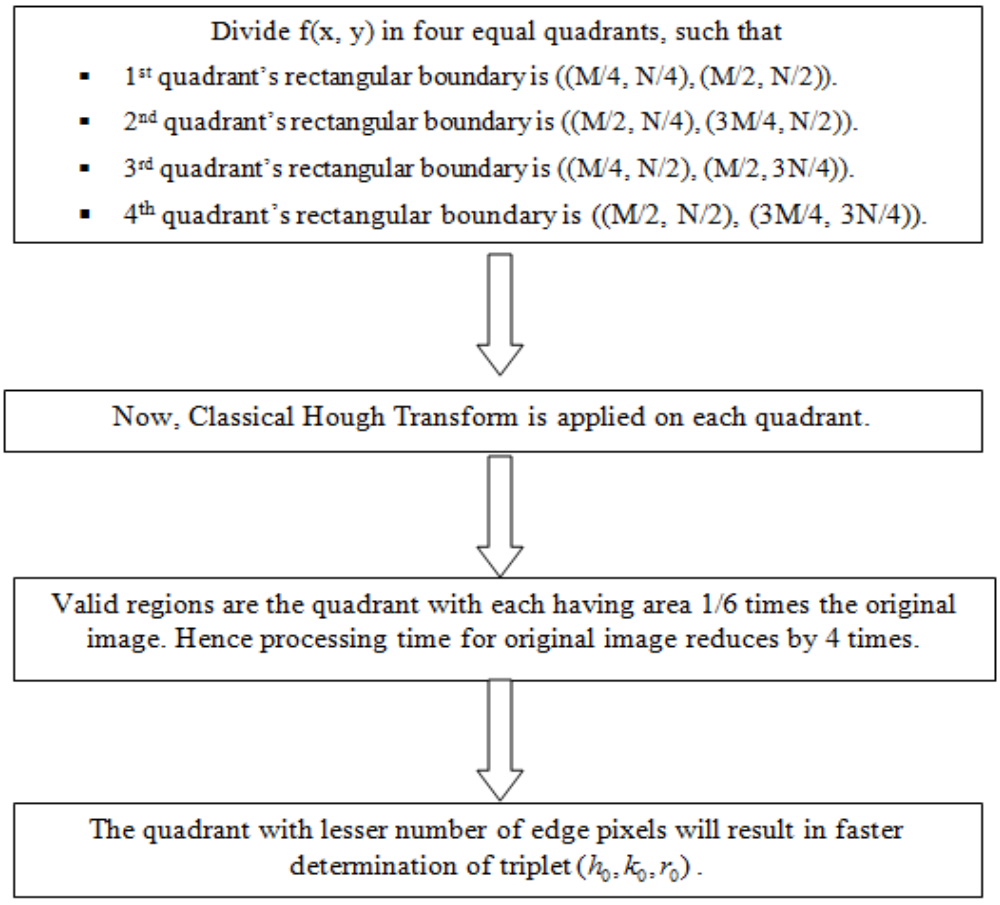

Figure 21: Graphical representation of Modified Classical Hough Transform

With the aim of improving time of existing CHT, the first step is devoted to obtain the valid region to process.

Following are the steps performed as preprocessing of CHT:

Step 1: The number of pixels to be processed is reduced using only four equal sized quadrants as shown in Figure 10 for finding center and radius of circle (iris).

Step 2: Let $f(x, y)$ be the image of size $M \times N$. Let A is the area of $f(x, y)$ then it is given by A $= M \times N$. Divide f(x, y) in four equal quadrants, such that, 1st quadrant's rectangular boundary is $((M/4, N/4), (M/2, N/2))$, 2nd quadrant's rectangular boundary is $((M/2, N/2), (3M/4, N/2))$, 3rd quadrant's rectangular boundary is $((M/4, N/2), (M/2, 3N/4))$, 4th quadrant's rectangular boundary is $((M/2, N/2), (3M/4, 3N/4))$.

Step 3: Now transformation is applied on each quadrant, the quadrant which contains lesser number of edge points will result in faster determination of triplet (h0, k0, r0). As clear from Figure 22, the valid regions are these quadrant with each having area 16 times lesser than original image. If A' is area of each quadrant then it is given by

$$A' = \frac{M}{4} \times \frac{N}{4} = \frac{A}{16}$$

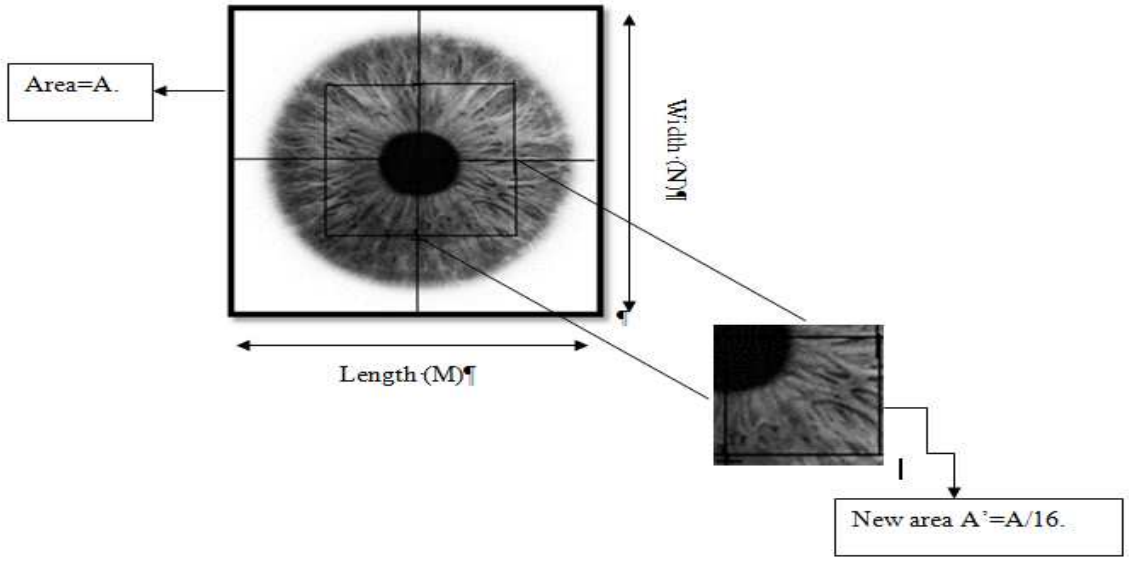

Figure 22: Reduction in area to be processed in Modified Classical Hough Transform.

Step 4: Now CHT can be performed on each such quadrant. Quadrant with lesser number of edge pixels will be processed faster and gives accurate results as other quadrants.

It reduces all the disadvantages of previous methods. In this method, valid region of image for iris recognition is fixed as a rectangular region which is most promising region in which center co-ordinates of iris circle could lie. That region separates legitimate region from illegitimate.

Assume an image containing iris, divided into four equal quadrants (Figure 20). This apparently reduces computational time and memory requirements. From that change of area, number of indices of accumulator array decreases and hence lesser no. of peaks or no. of votes appears to choose from.

From that, it's concluded that:

- Computationally fast.
- Less memory requirements.
- Easy to understand and implement.
- Recognition of valid region.
- Area to visit decreases by almost a factor of 16 for each time CHT runs.

CHAPTER 4-RESULTS AND COMPARISON

This chapter comprises of the comparative study of the proposed algorithm and existing CHT. This will provide an in-depth analysis of the fact that the proposed method is a better recognition algorithm than already existing CHT. To validate the script, experiment has been conducted on 100 images of human eye. The results of detected iris from the collected are shown in Table 2. The results so obtained are not all up to 100% accuracy. There are outputs which detect wrong center and radius. These inaccurate evaluations are caused by presence of eyelids in the image, angular displacement of iris, appearance of glare in the image captured etc.

4.1 Analysis of detected iris by CHT and MCHT

Table 2: Analysis of detected iris using CHT and MCHT.

Sno.	Original image	Output of CHT	Output of modified CHT
1.	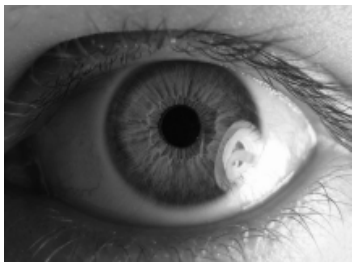		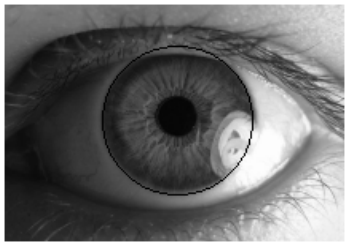
2.			

Sno.	Original image	Output of CHT	Output of modified CHT
3.		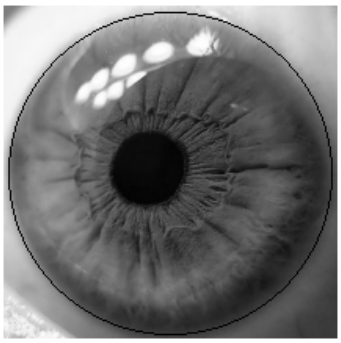	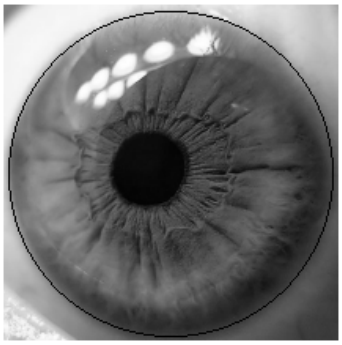
4.		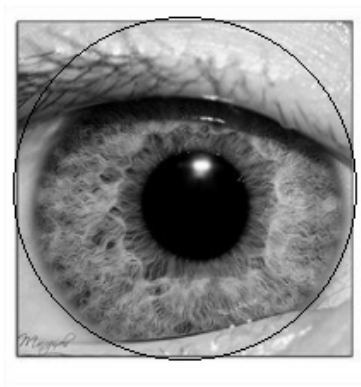	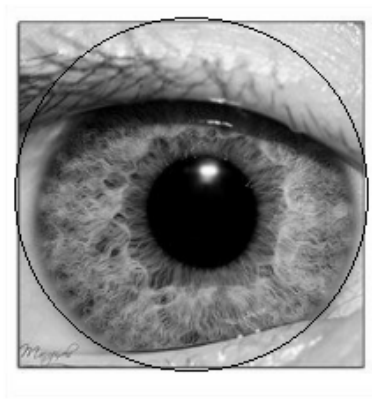
5.		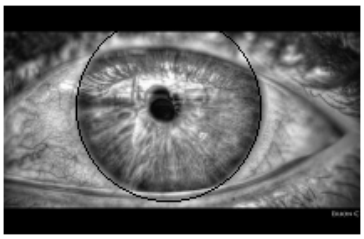	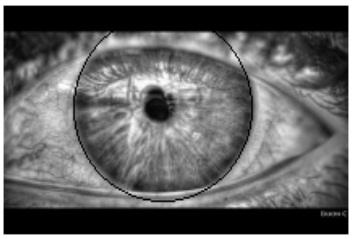
6.	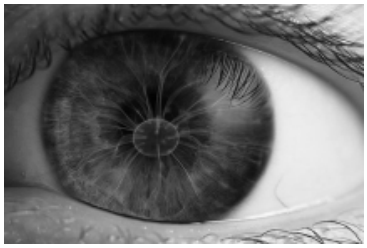	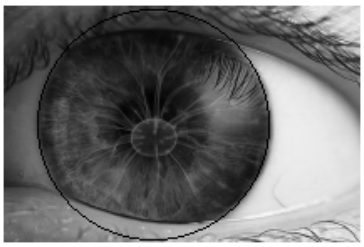	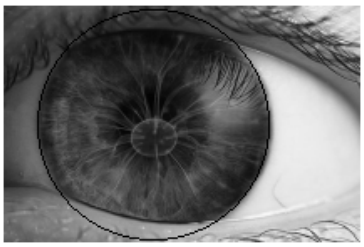

Sno.	Original image	Output of CHT	Output of modified CHT
7.	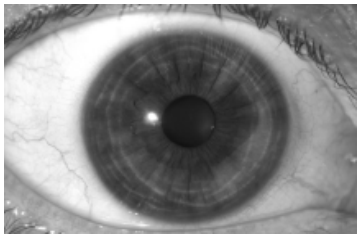	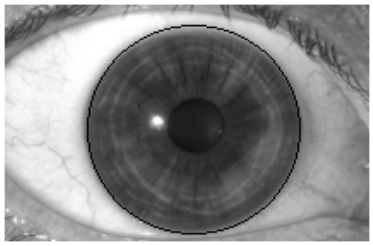	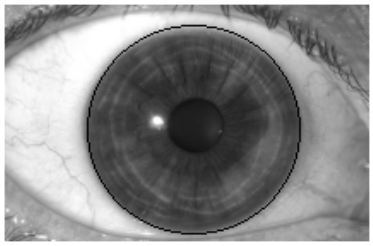
8.		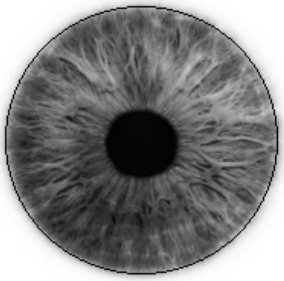	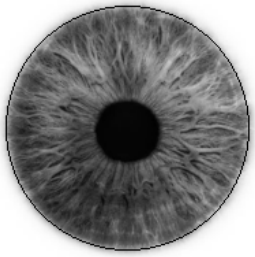
9.		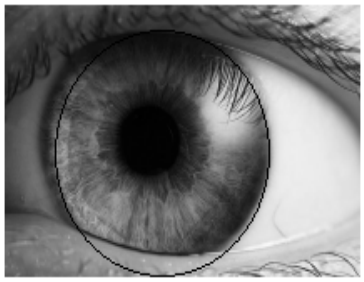	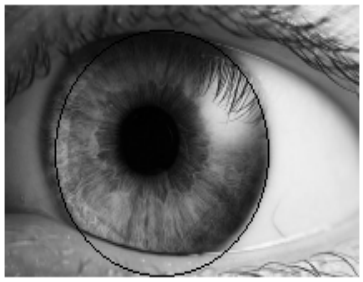
10.	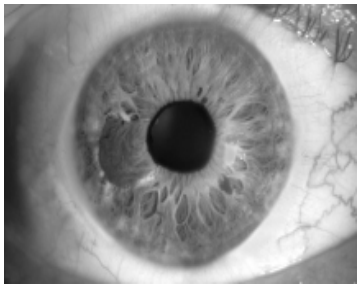		

Sno.	Original image	Output of CHT	Output of modified CHT
11.	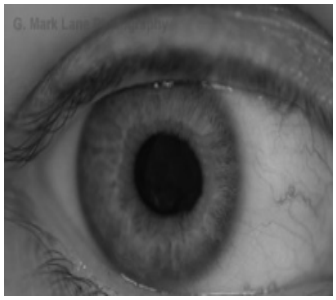	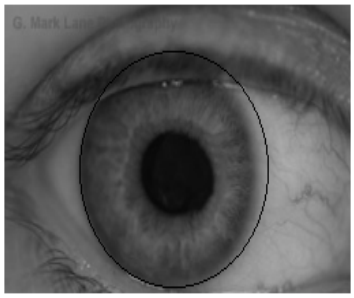	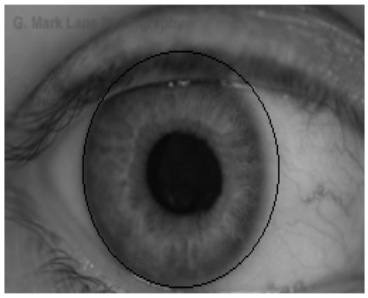
12.	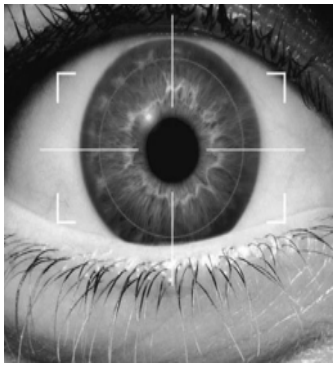	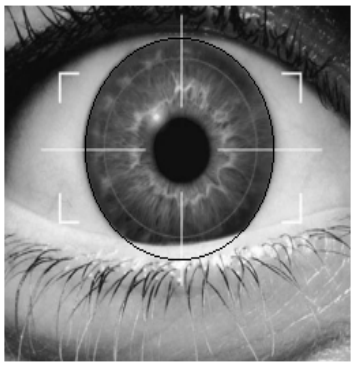	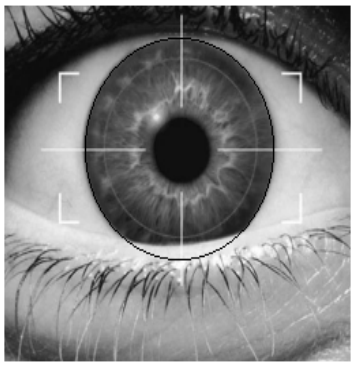
13.		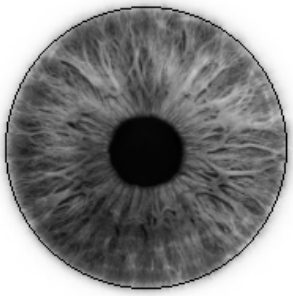	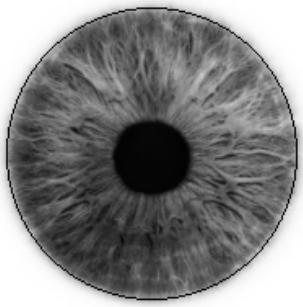
14.	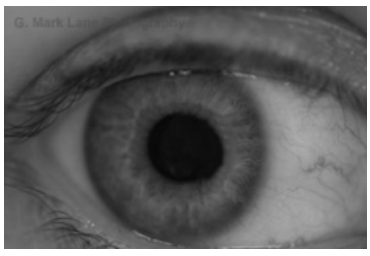	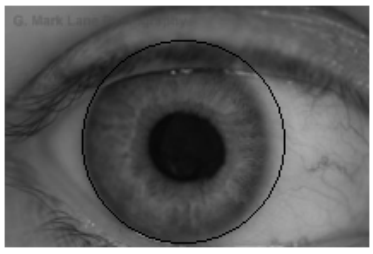	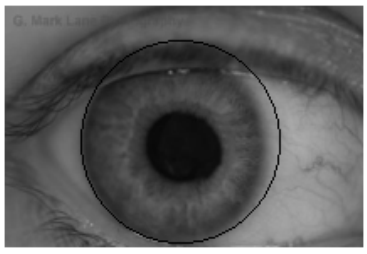

S.no.	Original image	Output of CHT	Output of modified CHT
15.	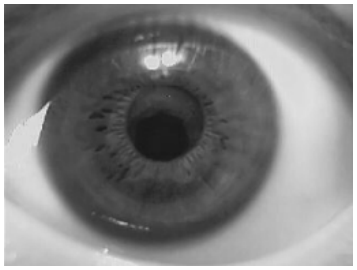		
16.	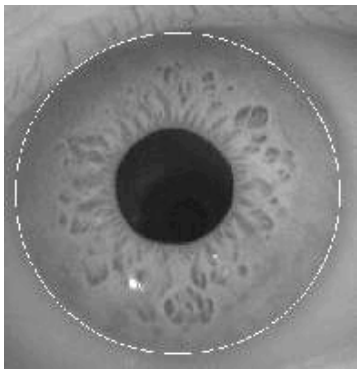	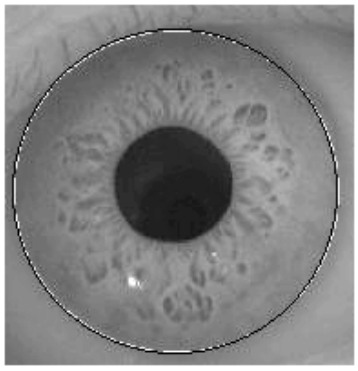	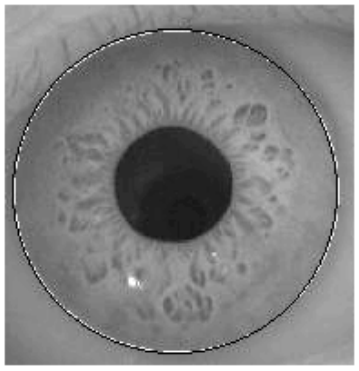
17.	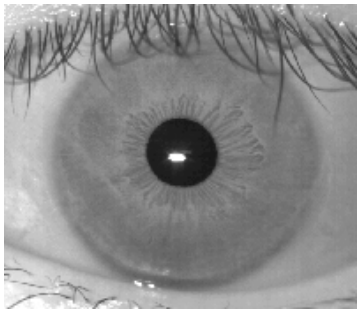	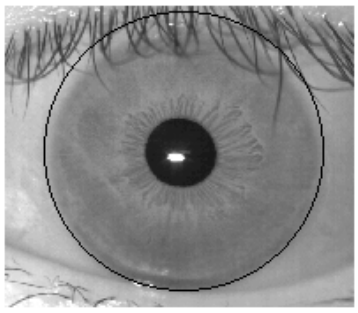	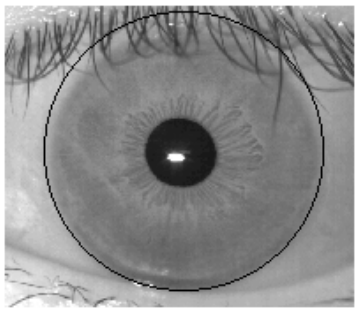
18.	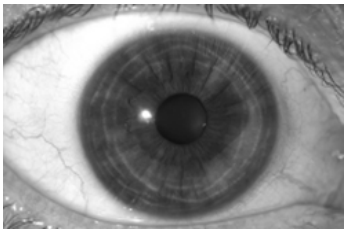	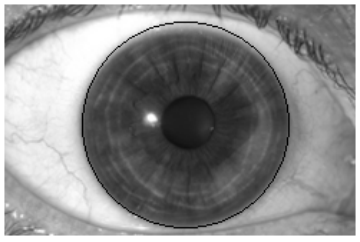	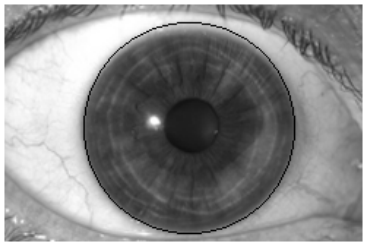

Sno.	Original image	Output of CHT	Output of modified CHT
19.	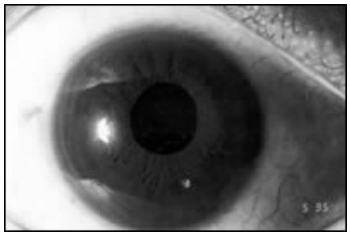		
20.		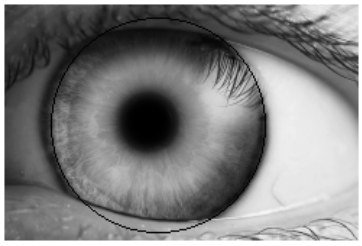	
21.	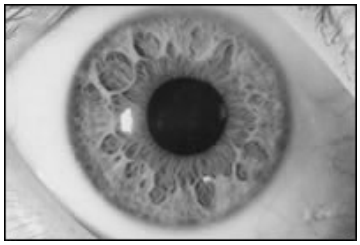	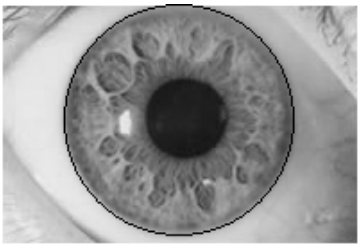	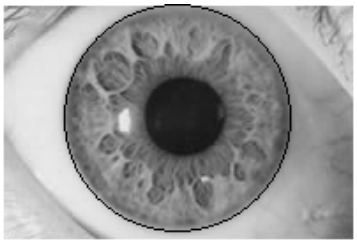
22.	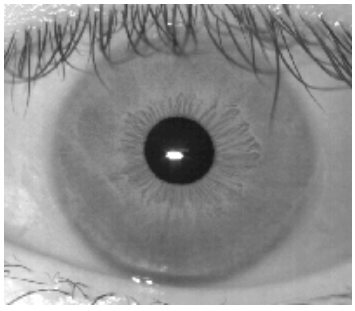	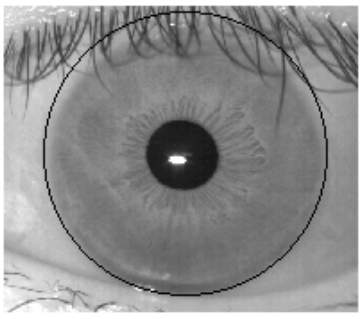	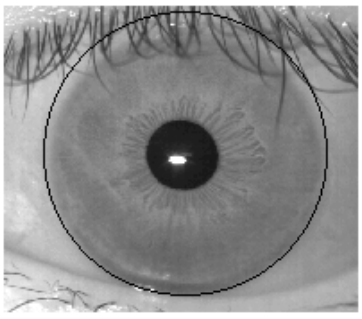

4.2 Analysis of time of execution of CHT and MCHT

Table 3 shows the efficiency of proposed method over existing CHT by comparing time of execution of both CHT and MCHT. Maximum efficiency show over an image is 97.33813947%. Table 4 shows comparison of the radius and center calculated by two methods. Numbers bold are the images which differ in result.

Table 3: Comparison of time of execution of CHT.

Name	Size	CHT [1]	MCHT	Efficiency of MCHT over CHT
		time(in sec)	time(in sec)	(%)
img_1	215x153	10.392	0.803	92.27290223
img_2	215x154	10.466	0.803	92.32753679
img_3	215x143	16.222	0.981	93.95265689
img_4	215x156	12.909	0.961	92.55558138
img_5	215x158	41.516	2.51	93.95413816
img_6	215x215	18.686	1.285	93.12319383
img_7	215x225	9.796	0.745	92.39485504
img_8	215x137	8.92	0.682	92.35426009
img_9	215x144	8.99	0.696	92.25806452
img_10	215x146	27.392	1.814	93.3776285
img_11	215x143	23.165	1.55	93.30887114
img_12	215x214	5.653	0.465	91.77427914
img_13	215x205	26.098	1.696	93.50141773
img_14	215x162	3.934	0.301	92.34875445
img_15	215x214	3.927	0.358	90.88362618
img_16	215x143	12.83	0.898	93.00077942
img_17	256x171	27.76	1.811	93.47622478
img_18	256x171	15.353	0.725	95.27779587
img_19	215x215	44.814	2.702	93.97063418

img_20	215x144	50.301	1.587	96.84499314
img_21	256x224	82.179	2.422	97.05277504
img_22	215x215	79.485	3.238	95.9262754
img_23	256x178	59.733	1.816	96.95980446
img_24	256x200	20.113	0.695	96.54452344
img_25	256x208	17.902	0.633	96.46408223
img_26	256x208	15.504	0.575	96.29127967
img_27	256x255	23.973	0.806	96.63788429
img_28	215x214	31.652	1.027	96.75533932
img_29	256x192	31.41	1.028	96.72715696
img_30	194x200	19.994	0.688	96.55896769
img_31	203x175	32.415	1.047	96.77001388
img_32	200x173	25.8	0.857	96.67829457
img_33	247x164	23.728	0.793	96.65795684
img_34	247x168	18.108	0.65	96.41042633
img_35	200x150	40.987	1.279	96.87949838
img_36	247x185	23.166	0.784	96.61572995
img_37	200x133	16.992	0.614	96.38653484
img_38	200x134	14.25	0.534	96.25263158
img_39	247x204	22.762	0.781	96.56884281
img_40	247x186	23.87	0.796	96.66527021
img_41	250x170	40.761	1.28	96.85974338
img_42	247x165	17.245	0.634	96.32357205

img_43	215x161	14.321	0.536	96.25724461
img_44	200x150	51.159	1.666	96.74348599
img_45	200x150	79.914	2.541	96.82033186
img_46	215x143	86.35	3.249	96.23740591
img_47	247x165	57.918	1.904	96.71259367
img_48	215x177	17.307	0.698	95.96694979
img_49	215x162	21.639	0.576	97.33813947
img_50	215x146	30.76	1.033	96.64174252
	MAXIMUM PERFORMANCE			97.33813947
	AVERAGE PERFORMANCE			94.45732238
	MINIMUM PERFORMANCE			92.27290223

Table 4: Comparison of the radius and center of iris calculated by CHT and MCHT.

Name	size	CHT [1]		MCHT	
		Center	radius	Center	radius
img_1	215x153	95,78	64	**98,74**	**60**
img_2	215x154	95,74	64	**94,70**	**65**
img_3	215x143	95,78	64	**95,78**	**65**
img_4	215x156	107,108	104	**107,108**	**105**
img_5	215x158	107,108	99	107,108	99

img_6	215x215	99,61	55	99,61	55
img_7	215x225	90,68	70	90,68	70
img_8	215x137	111,78	65	**111,72**	**68**
img_9	215x144	111,75	62	111,75	62
img_10	215x146	110,106	89	110,106	89
img_11	215x143	110,102	85	110,102	85
img_12	215x214	134,97	43	134,97	43
img_13	215x205	110,106	89	110,106	89
img_14	215x162	126,96	70	135,83	85
img_15	215x214	126,96	70	126,96	70
img_16	215x143	143,87	46	169,83	60
img_17	256x171	129,108	97	129,108	97
img_18	256x171	108,69	65	108,69	65
img_19	215x215	128,92	70	128,92	70
img_20	215x144	109,112	97	109,112	97
img_21	256x224	124,84	70	124,84	70
img_22	215x215	131,128	106	131,128	106
img_23	256x178	110,106	89	110,106	89
img_24	256x200	113,91	87	113,91	87
img_25	256x208	95,103	89	95,103	89
img_26	256x208	106,84	80	106,84	80
img_27	256x255	94,91	89	94,91	89
img_28	215x214	126,85	72	126,85	72

img_29	256x192	128,90	76	128,90	76
img_30	194x200	112,77	70	112,77	70
img_31	203x175	114,86	82	114,86	82
img_32	200x173	135,60	75	135,60	75
img_33	247x164	137,84	82	137,84	82
img_34	247x168	96,78	65	96,78	65
img_35	200x150	123,79	78	123,79	78
img_36	247x185	116,95	101	116,95	101
img_37	200x133	124,51	72	124,51	72
img_38	200x134	119,70	72	119,70	72
img_39	247x204	90,72	68	90,72	68
img_40	247x186	137,84	82	137,84	82
img_41	250x170	123,79	78	123,79	78
img_42	247x165	124,51	72	124,51	72
img_43	215x161	119,70	72	119,70	72
img_44	200x150	109,112	97	109,112	97
img_45	200x150	124,84	70	124,84	70
img_46	215x143	131,128	106	131,128	106
img_47	247x165	110,106	89	110,106	89
img_48	215x177	95,103	89	95,103	89
img_49	215x162	141,141	140	141,141	140
img_50	215x146	126,85	72	126,85	72

4.3 Analysis of graphical comparison between CHT and MCHT

Figure 38 shows the graphical representation of efficiency of CHT and modified CHT. It clearly shows the difference in peaks of time of execution of CHT and modified CHT.

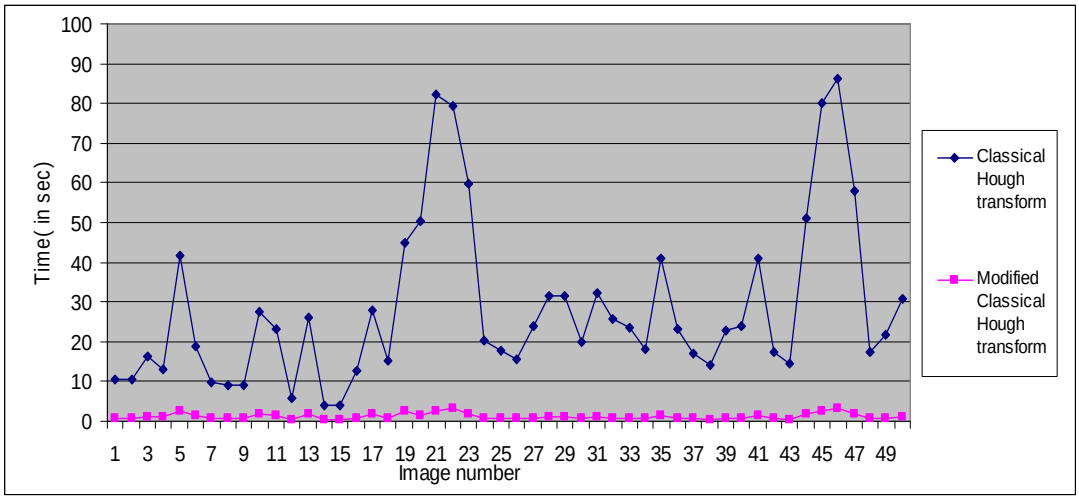

Figure 23: Graphical comparison of time of execution of CHT and MCHT.

4.4 Comparison and discussion

If the input image Figure 24 is say img_7 and the output image Figure 25 say img_7_cht is the image showing result of circle detection by CHT then

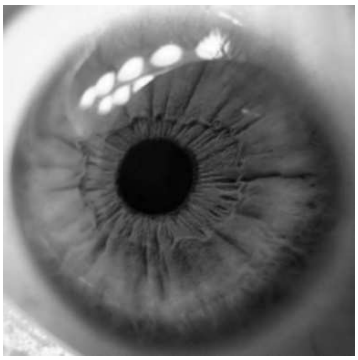

Figure 24: Sample input image img_7.tif.

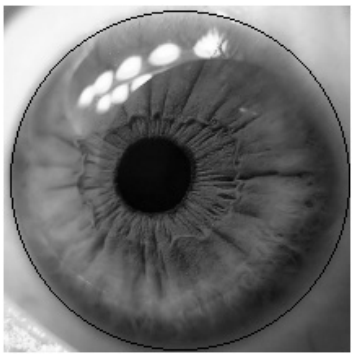

Figure 25: Sample output image img_7_cht.tif.

Figure 34 shows that the time taken by CHT to detect circle center and radius is 33.983 seconds. It's clear from the Figure 36 that time taken by modified CHT is 2.45 seconds. This shows an efficiency of 93.95413816%. Also, the results show that both detected the same center and radius co-ordinates. If img_7.tif is input image, then output of modified CHT is

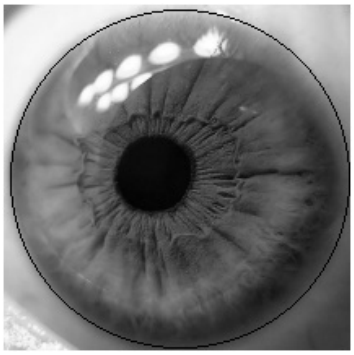

Figure 26: Sample output image img_7_mcht.tif.

On comparing CHT with modified CHT, it clearly shows a great amount of reduction in execution time. Hence, it shows the maximum improvement of about 96.64174252%. On an average, its performance increases by 94.45732238%.

Table 5 shows various differences between existing and proposed CHT on the basis of time to execute, space required to store data, and implementation complexity.

Table 5: Comparison of CHT and MCHT.

NAME OF METHOD	COMPUTATIONAL TIME	SPACE REQUIREMENTS	IMPLEMENTATION COMPLEXITY
CHT	**HIGH**	**HIGH**	**MODERATE**
MCHT	**LOW**	**LOW**	**LOWER**

CHAPTER 5-CONCLUSION & FUTURE SCOPE

5.1 Concluding remarks

Modified CHT for detection of circle from digital images suitable for iris images are proposed. A complete analysis of classical method and proposed method is obtainable. HT based algorithms are time consuming and use quite large memory for data storage. In addition to it, execution speed of HT based detection methods is directly proportional to the number of edge pixels in the input image. The proposed method reduces the number of image edge pixels to be processed at a time using the smaller quadrants hence increasing the efficiency of detection as well. The gain in efficiency does not affect the robustness of the techniques. These advantages make the algorithms most suitable for applications where iris location detection is a critical aspect. To validate the script, a data set of 100 images of human eye is evaluated. The results of detected iris from the collected data set are shown in Table 2. The results so obtained are not up to 100% accuracy. There are outputs which detect wrong center and radius. These inaccurate evaluations are caused by presence of eyelids in the image, angular displacement of iris, appearance of glare in the image captured etc.

5.2 Future scope

The development of thesis **"Robust and accurate Classical Hough Transform approach for IRIS recognition"** is original and creative. The final outcome of this experience was the implementation and analysis of a novel iris recognition algorithm. Future designs may tackle real time imaging. That is, images are taken continuously as the person approaches system for identification and thus identified under no cooperation from the user. Presented work can also be done to come up with better techniques that enable the system to detect the eyelids and eyelashes and remove them from the iris region to limit errors. Also, this work can also proceed towards handling eye placing angle at the device to detect eyes and finding best frame to capture eye for detecting iris

in faster and accurate way.

APPENDIX -I

Implementation details of existing Classical Hough Transform (CHT): we start by opening the program in Microsoft visual C++.

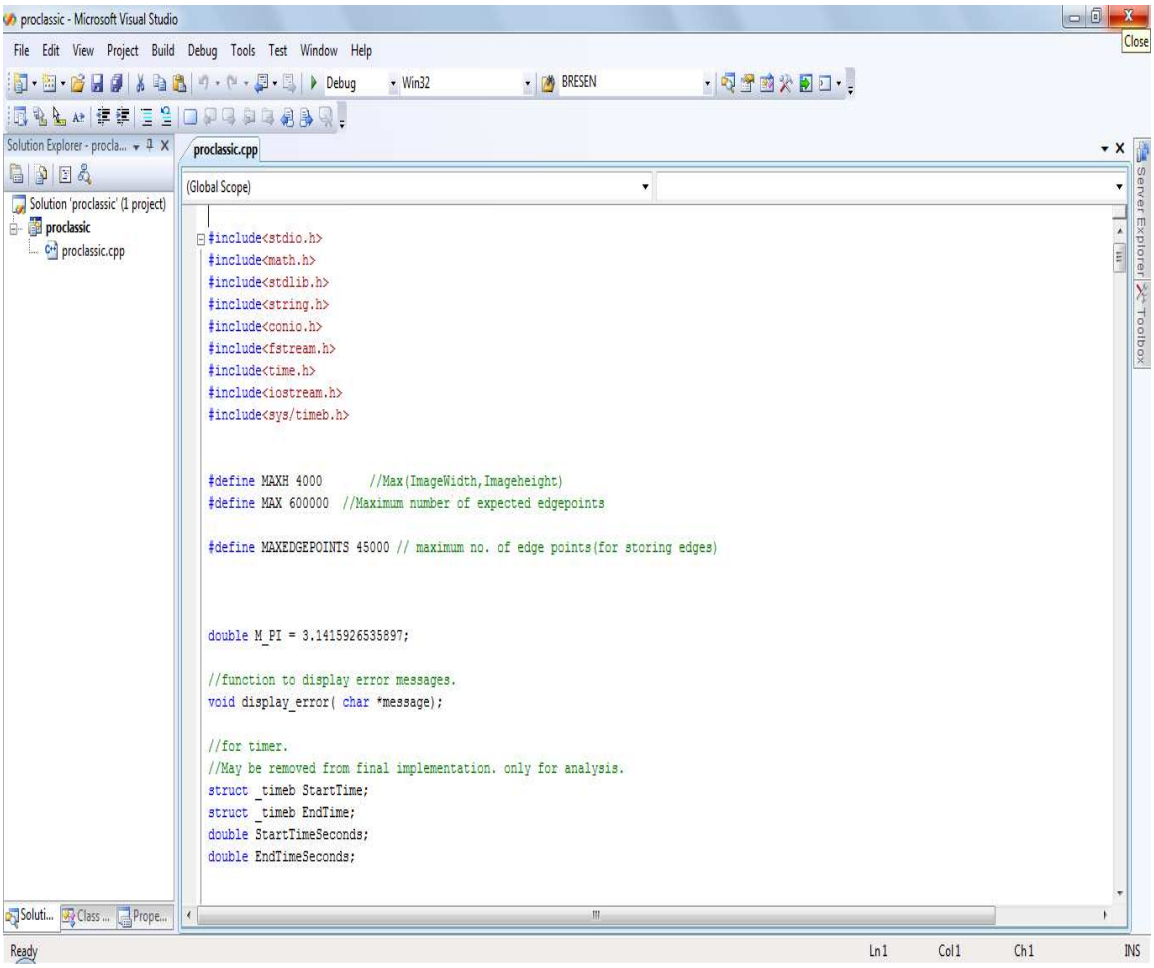

Figure 27: CHT program code.

Execution of the program begins by:

- Creating a build

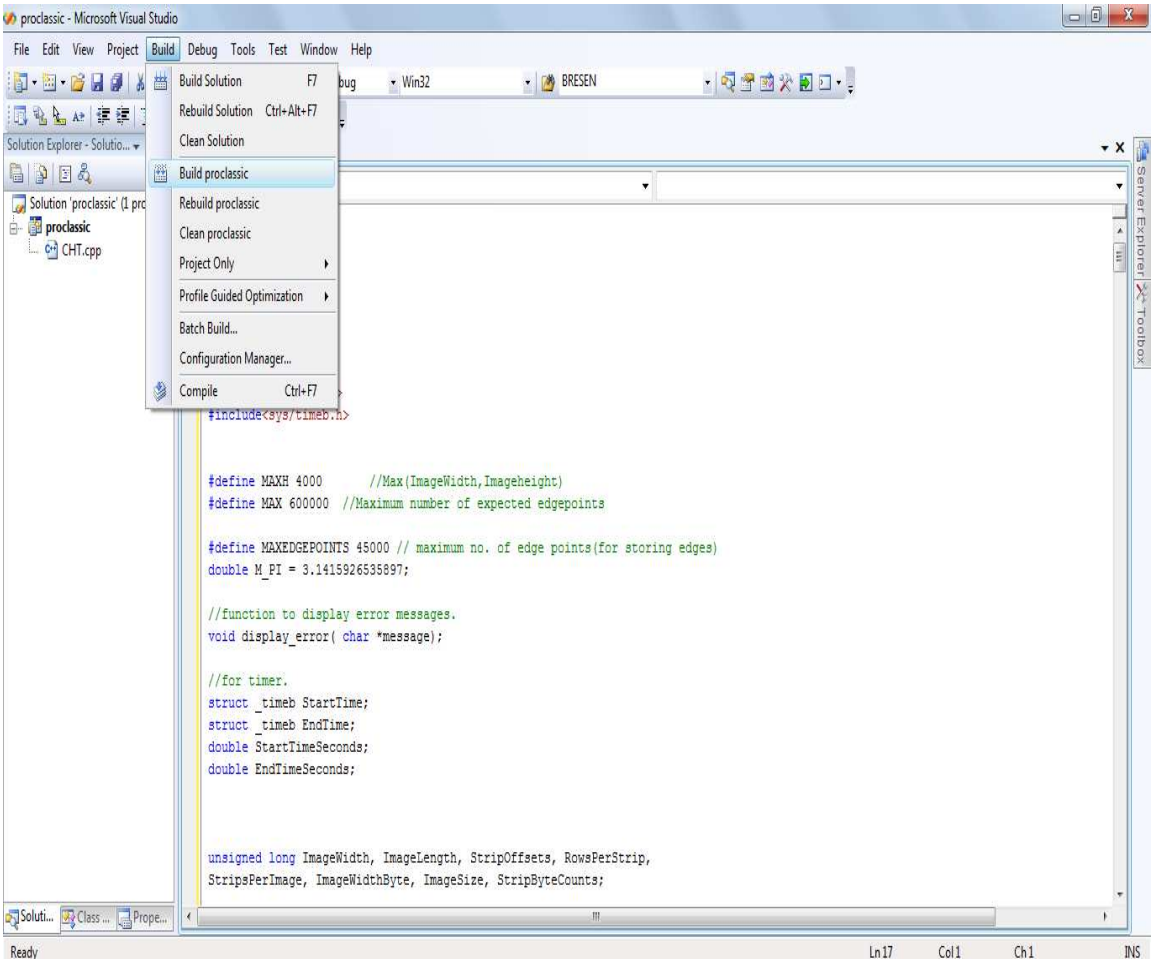

Figure 28: Creating a build.

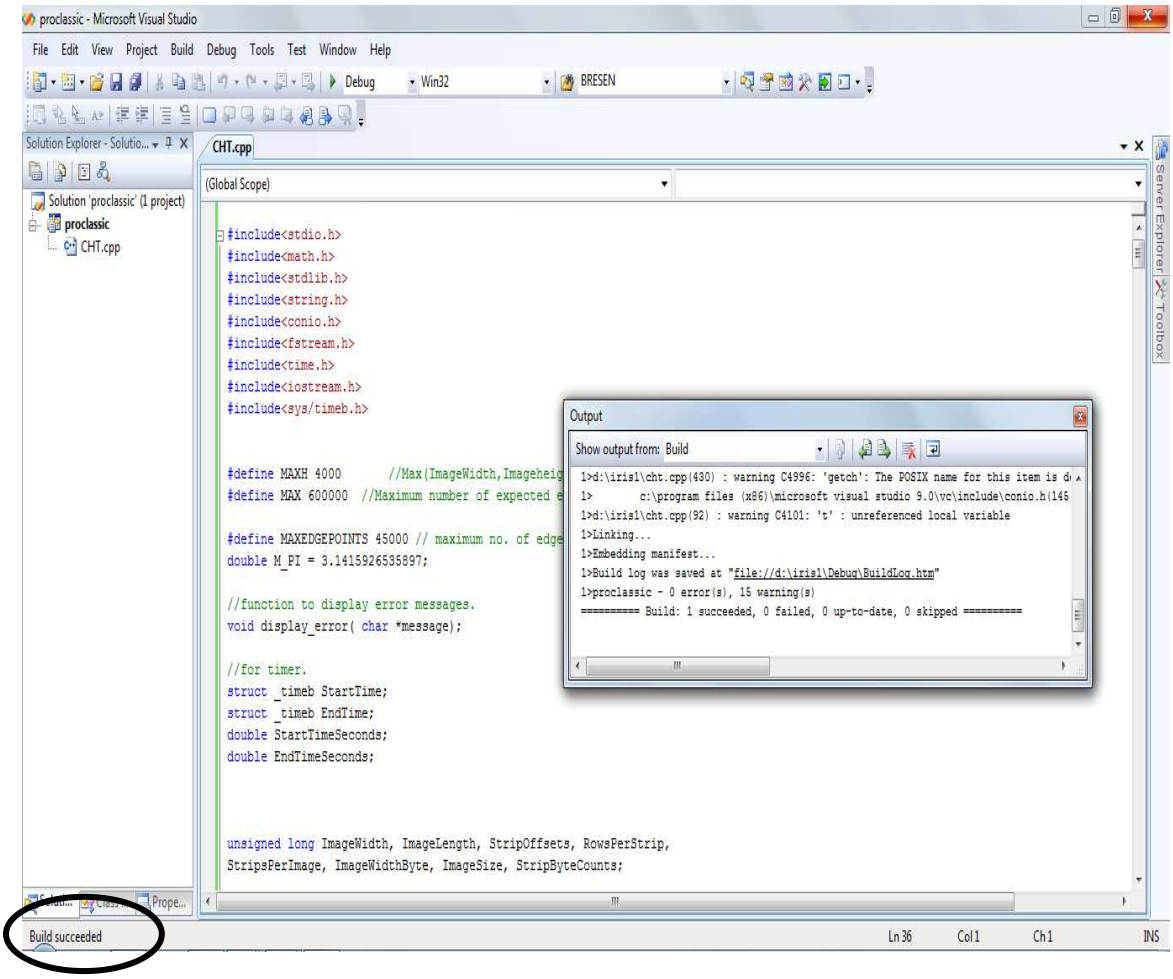

Figure 29: Successful build creation.

- Once build is success, start debugging the code.

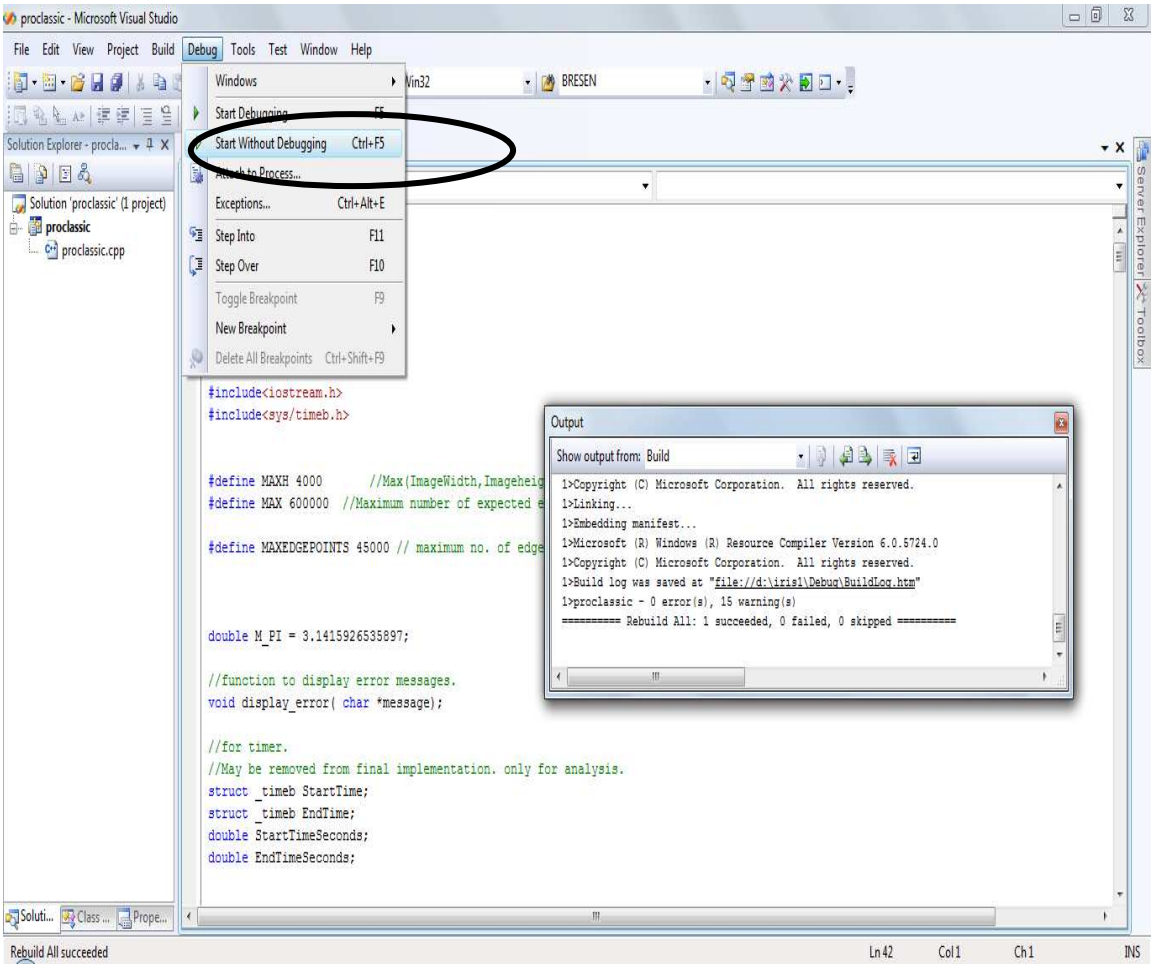

Figure 30: Debug the code.

- Command prompt appears for the final execution step of the code.

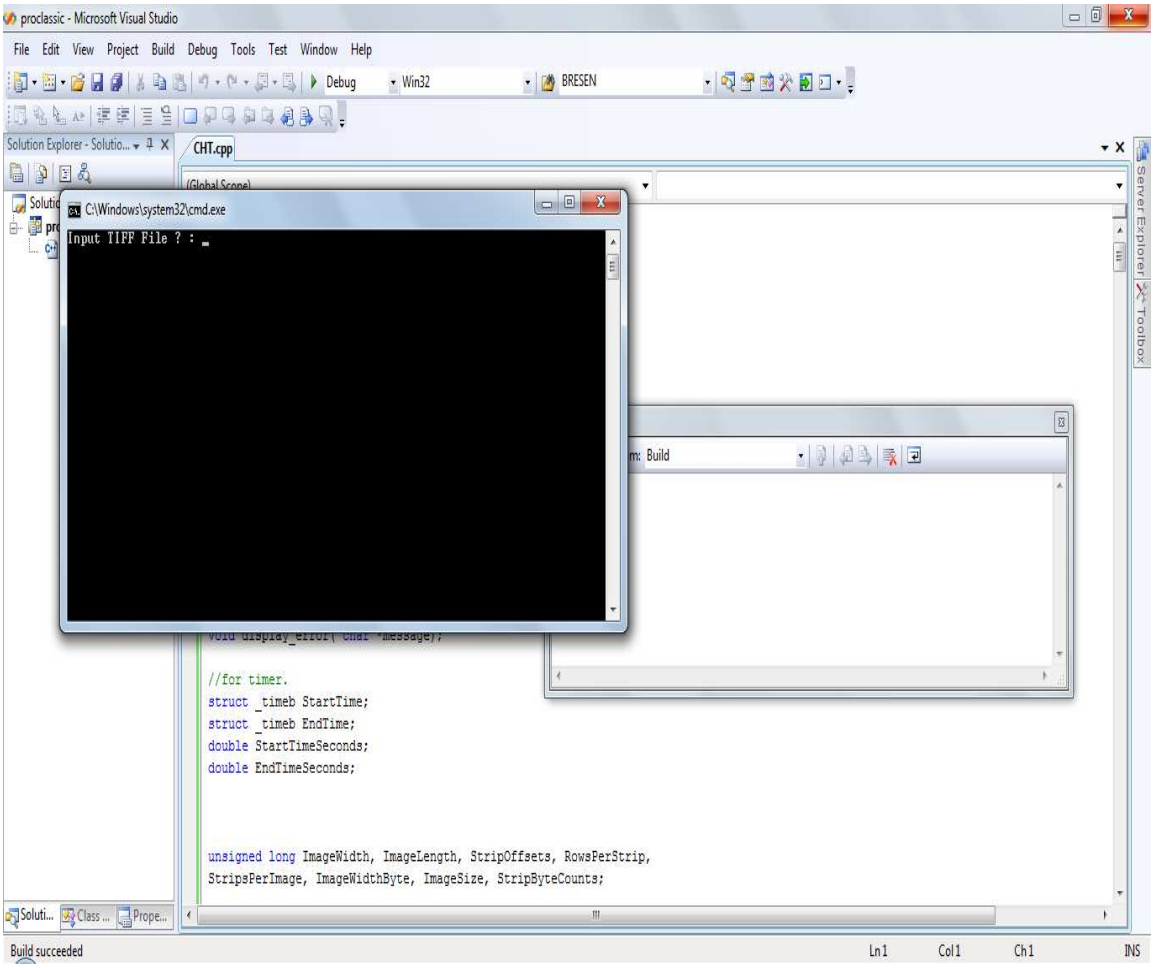

Figure 31: Command prompt after successful debugging.

- In the command prompt, the basic first step is to give input file that correspond to the gray scale image containing iris.

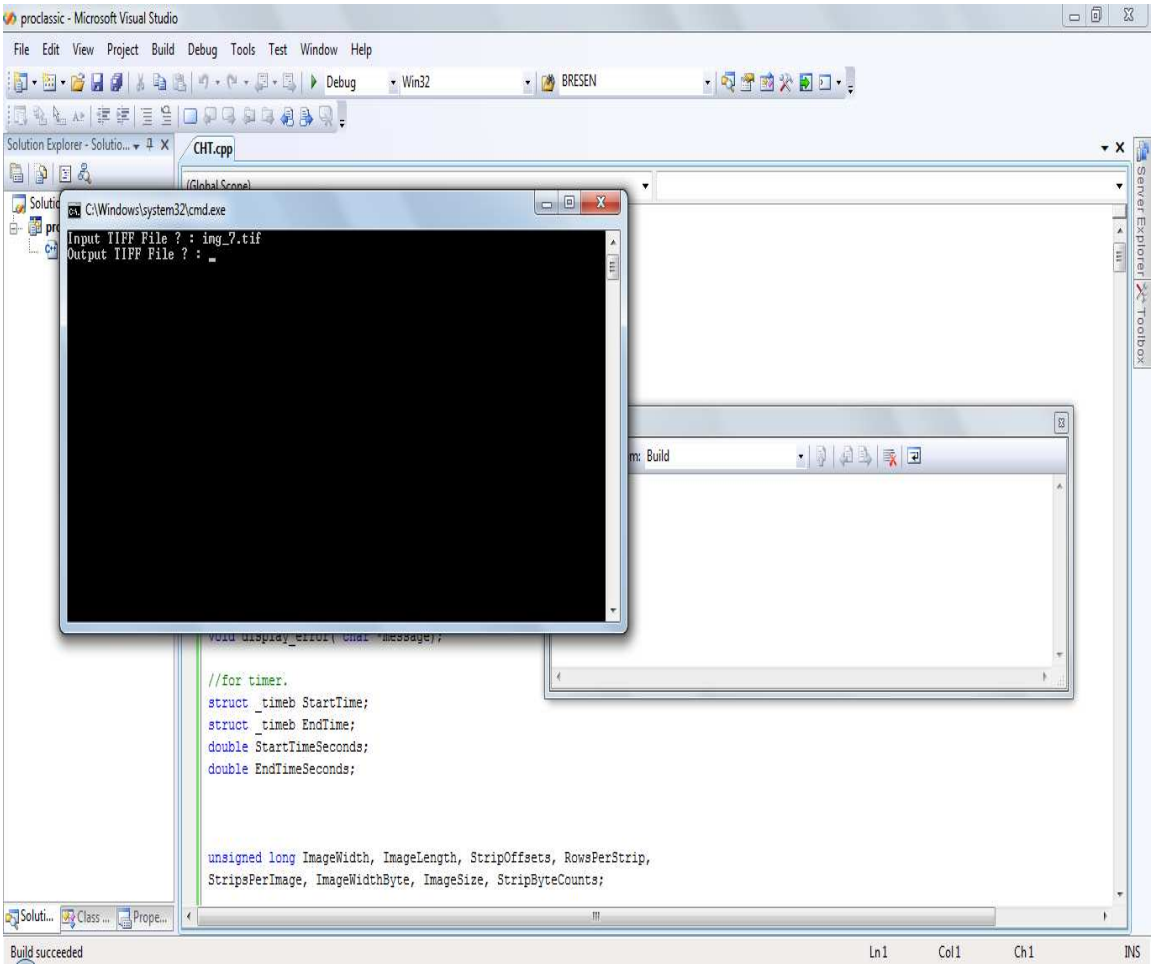

Figure 32: Entering input file for iris detection.

- Next step is to give name of the output file where the image with detected iris is to be stored.

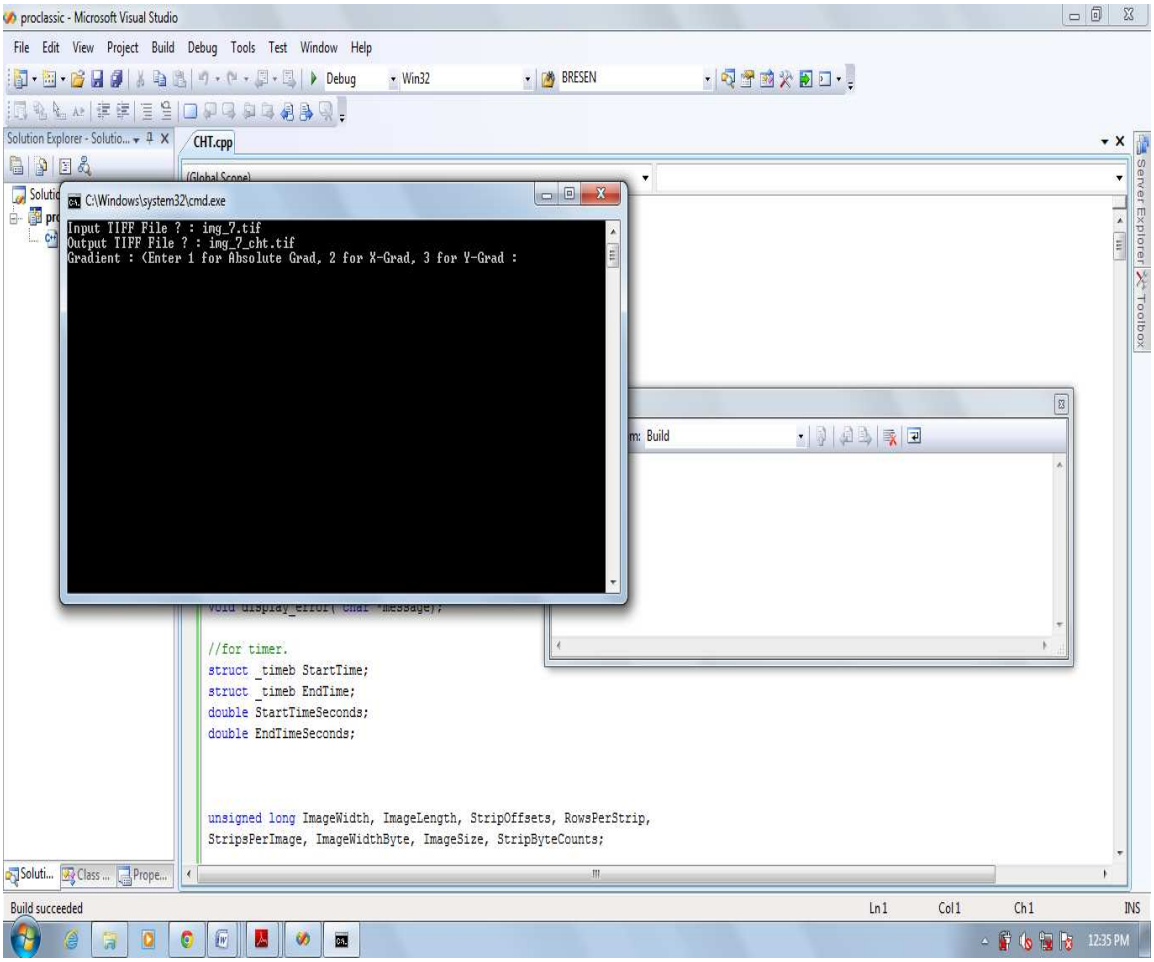

Figure 33: Entering output file for iris detection.

- After the output file is given a name, code executes and returns image properties. In addition to it, it also returns center and radius of iris detected and the time taken to detect the same as shown in Figure 34.

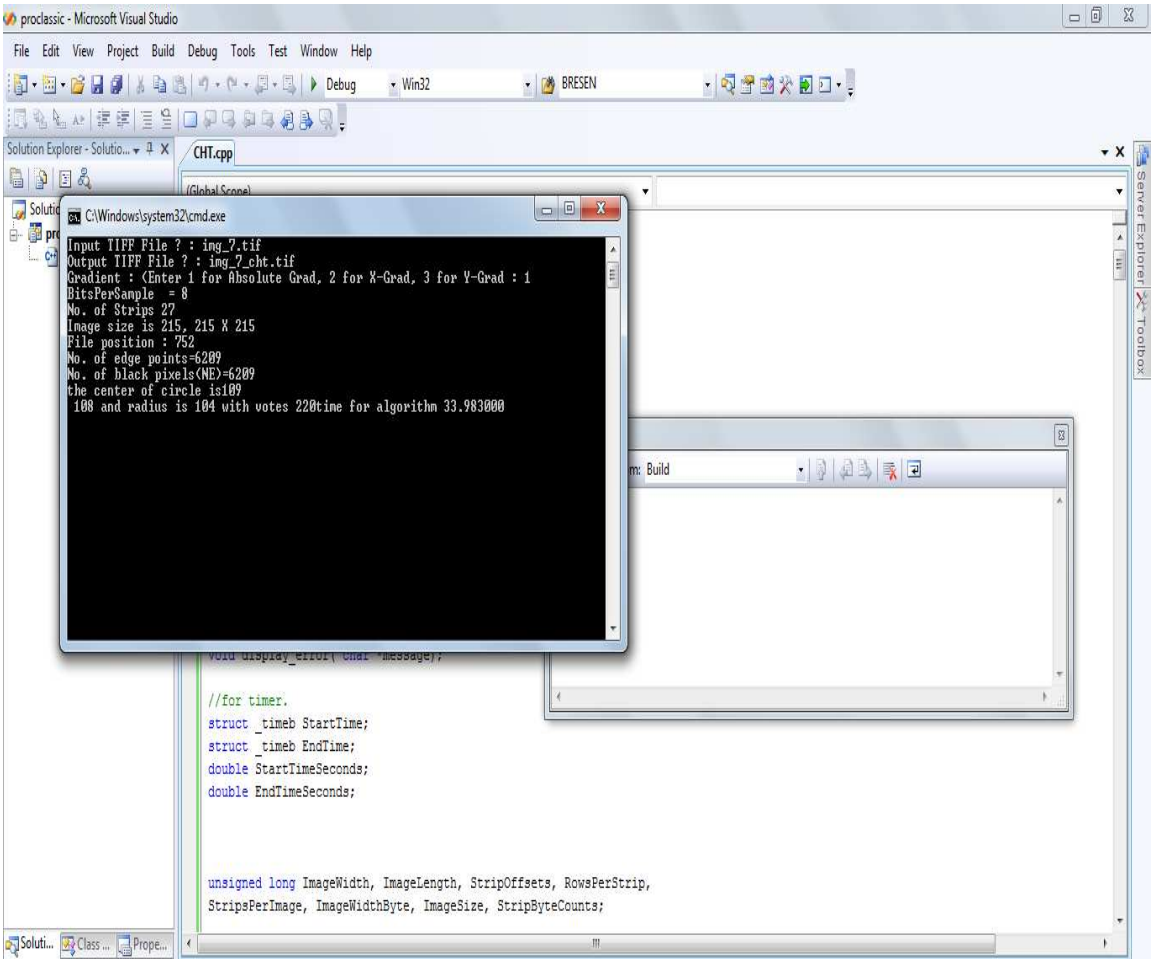

Figure 34: Center and radius co-ordinates with time taken to detect it.

Now steps to detect circle by modified CHT are as follows:

- Open code of modified CHT in Microsoft Visual C++.
- Build it and after a success, debug it.

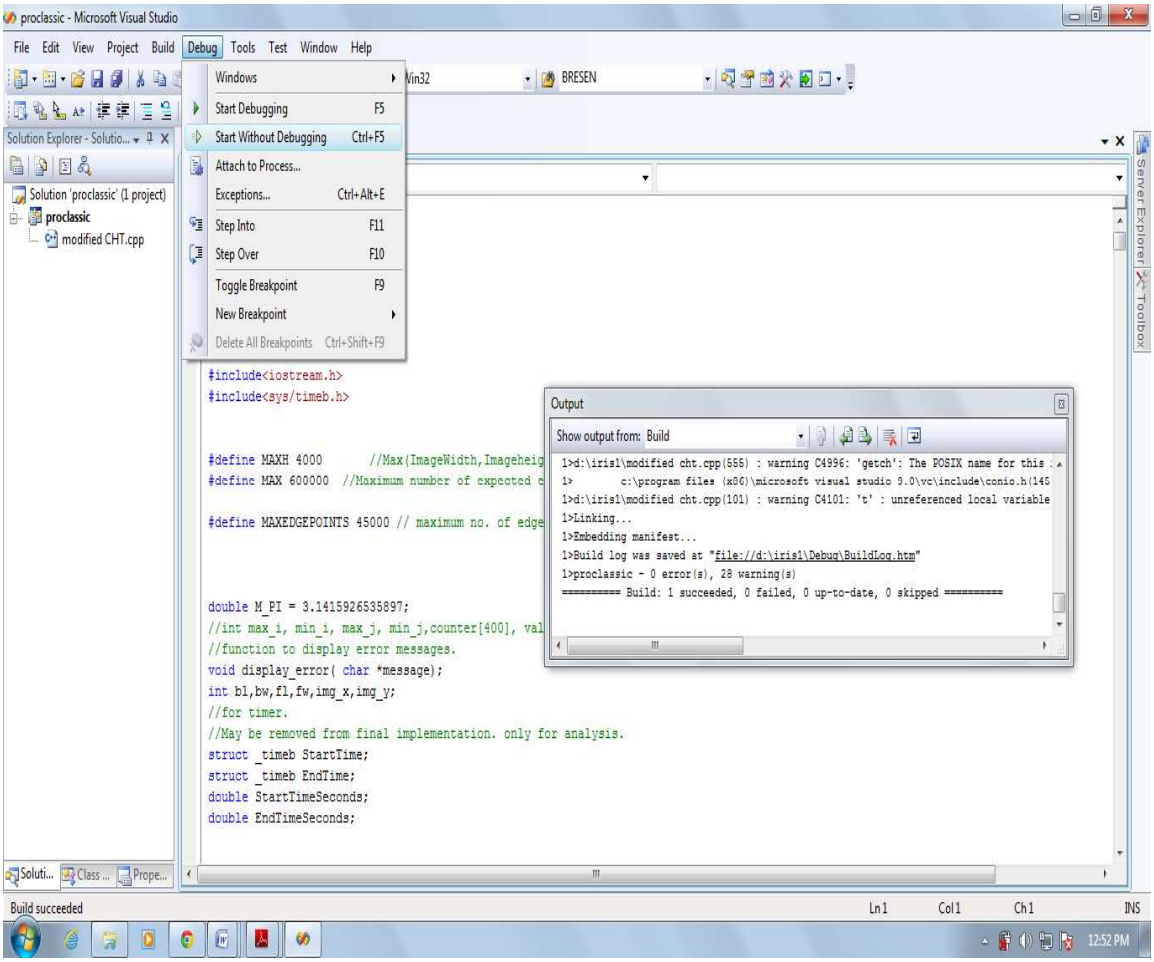

Figure 35: Modified code for debugging.

- Enter input image file as img_7.tif and output image file as img_7_mcht.tif in order to compare results. Now check the time of execution and at same time the center and radius calculated.

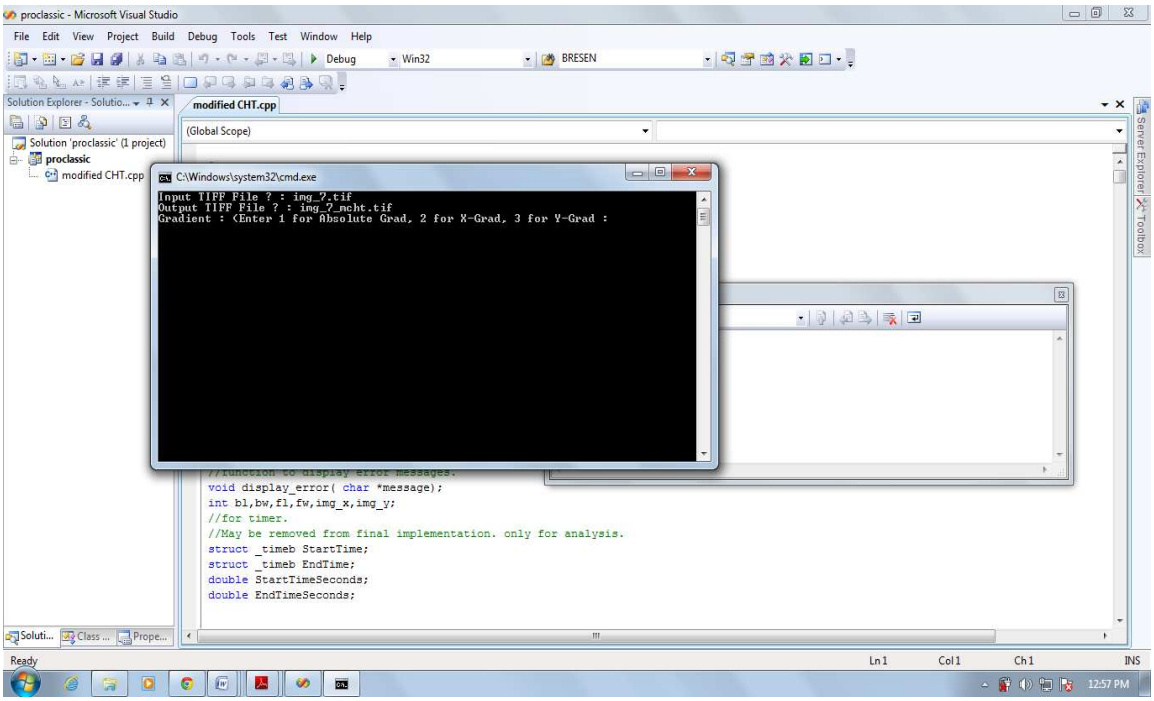

Figure 36: Output image as img_7_mcht.tif.

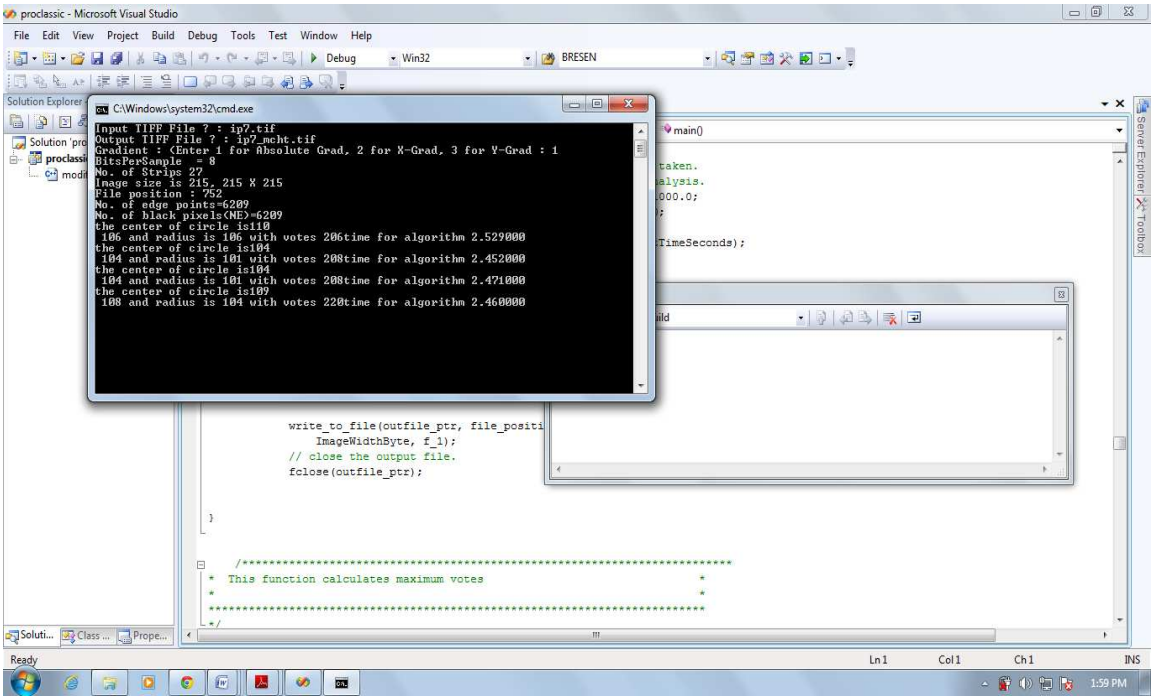

Figure 37: Results of modified CHT.

BIBLIOGRAPHY

[1]. R. Duda and P. Hart, Use of Hough transform is to detect lines and curves in pictures, Communications of the ACM 15, (1975), 11-15.

[2]. S. Tsuji, F. Matsumoto, Detection of ellipses by a modified Hough Transformation, IEEE Transactions on Computers, (1978) 777-781S.

[3]. K. Shearer, L. Kitchen, Filling gaps in the Hough-transform voting locus for N-dimensional parameter spaces, Pattern Recognition Letters 16 (1995) 1105-1109.

[4]. D. Walsh, A. Raftery, Accurate and efficient curve detection in images: the importance sampling Hough transforms, Pattern Recognition, (2002), 1421-1431.

[5]. J. Cha, R.H. Cofer, S.P. Kozaitis, Extended Hough transform for linear feature detection, Pattern Recognition, (2006), 1034-1043.

[6]. S. Sekhar, W. Al-Nuaimy A.K. Nandi, Automated localisation of retinal optic disk using Hough transform, 5th IEEE International Symposium on Biomedical Imaging: From Nano to Macro, 1577-1580.

[7]. G. Reina, G. Ishigami, K. Nagatani, K Yoshida, Vision-based estimation of slip angle for mobile robots and planetary rovers IEEE International Conference on Robotics and Automation (2008). 486-491.

[8]. L. Fernandes, M. Oliveira, Real-time line detection through an improved Hough transform voting scheme, Pattern Recognition, (2008), 299-314.

[9]. H. Zhao, A. W. Liew, X. Xie, H. Yan, A new geometric biclustering algorithm based on the Hough transform for analysis of large-scale microarray data, Journal of Theoretical Biology, (2008), 264-274.

[10]. W. Lu, J. Tan, Detection of incomplete ellipse in images with strong noise by iterative randomized Hough transform (IRHT), Pattern Recognition, (2008), Pages 1268-1279.

[11]. M. Smereka and I. Duleba, Circular object detection using a modified hough transform, Int. J. Appl. Math. Comput. Sci., (2008), 85-91.

[12]. C. Singh, N. Bhatia, A. Kaur, Hough transform based fast skew detection and accurate skew correction methods, Pattern Recognition(2008), 3528-3546.

[13]. W. Du, J. Yang, A robust Hough transform algorithm for determining the radiation centers of circular and rectangular fields with subpixel accuracy, Phys. Med. Biol. (2009) 555-567.

[14]. S. Maji, J. Malik, Object Detection using a Max-Margin Hough Transform, Computer Vision and Pattern Recognition, (2009) 1038-1045.

[15]. R.Bansal, P. Arora, M. Gaur, P. Sehgal, P Bedi, Fingerprint Image Enhancement Using Type-2 Fuzzy Sets, Sixth International Conference on Fuzzy Systems and Knowledge Discovery, (2009)., 412-417.

[16]. J. Gall, V. Lempitsky, Class-specific Hough forests for object detection, IEEE Conference on Computer Vision and Pattern Recognition, (2009), 1022-1029.

[17]. S. Guo, T. Pridmore, Y. Kong, X. Zhang, An improved Hough transform voting scheme utilizing surround suppression, Pattern Recognition Letters, (2009), 1241-125.

[18]. H.D. Cheng, Y. Guo, Y. Zhang, A novel Hough transform based on eliminating particle swarm optimization and its applications, Pattern Recognition, (2009), 1959-1969.

[19]. H. Izadinia, F. Sadeghi, M. Ebadzadeh, Fuzzy generalized hough transform invariant to rotation and scale in noisy environment, IEEE International Conference on Fuzzy Systems FUZZ-IEEE (2009), 153-158.

[20]. D. Borrmann, J. Elseberg, K. Lingemann, A. Niichter, A Data Structure for the 3D Hough Transfrom for Plane Detection, 7th IFAC Symp. Intell. Aut. Vehicles (2010).

[21]. H. Ruppertshofen, C. Lorenz, P. Beyerlein, Z. Salah , G. Rose, H. Schramm Fully automatic model creation for object localization utilizing the Generalized Hough transform, Bildverarbeitung fr die Medizin. Springer, (2010) 281-285.

[22]. J. Knopp, M. Prasad, G. Willems, R. Timofte, L. Van Gool, Hough transform and 3d surf for robust three dimensional classification, ECCV, (2010).

[23]. N.Bhatia, M. Chhabra, Improved Hough transform for fast iris detection, Proceedings on International Conference on Signal Processing Systems, Dalian (2010), 172-176.

[24]. A. Maki, F. Perbet, B. Stenger, Demisting the Hough transform for 3D shape recognition and registration, BMVC, 2011.

[25]. C.Tu, S. Du, B.J. Van Wyk, K. Djouani, Y. Hamam, , High resolution Hough transform based on buttery self-similarity, Electronics Letters , (2011),1360-1361.

[26]. F. Mokhayeri, M.R Akbarzadeh, Mental Stress Detection Based on Soft Computing Techniques, IEEE International Conference on Bioinformatics and Biomedicine (BIBM), (2011), 430-433.

[27]. A. Lehmann, B. Leibe, LV. Gool , Fast prism: Branch and bound Hough transform for object class detection, International Journal of Computer Vision, (2011), 175-197.

[28]. T.Y. Lee, T.S. Chang, S.H. Lai, K.C. Liu, H.S. Wu, Wide-angle distortion correction by Hough transform and gradient estimation, IEEE Visual Communications and Image Processing (VCIP), 2011, 1-4.

[29]. http://homepages.inf.ed.ac.uk/rbf/HIPR2/hough.htm

[30]. http://www.scantips.com/basics9t.html

[31]. The Handbook of Pattern Recognition and Computer Vision (2nd Edition), by C.H. Chen, L. F. Pau, P. S. P. Wang (eds.), World Scientific Publishing Co.

50….70….

Results, table..conclusion..